Resonance in a model for Cooker's sloshing experiment

— the extended version —

by H. Alemi Ardakani, T.J. Bridges & M.R. Turner

Department of Mathematics, University of Surrey, Guildford, Surrey GU2 7XH, England

– Abstract –

Cooker's sloshing experiment is a prototype for studying the dynamic coupling between fluid sloshing and vessel motion. It involves a container, partially filled with fluid, suspended by two cables and constrained to remain horizontal while undergoing a pendulum-like motion. In this paper a fully-nonlinear model is developed for the coupled system. The Euler equations relative to a moving frame govern the fluid motion, and the vessel motion is a forced nonlinear pendulum equation. The equations are then linearized and the natural frequencies studied. The coupling leads to a highly nonlinear transcendental characteristic equation for the frequencies. Two derivations of the characteristic equation are given, one based on a cosine expansion and the other based on a class of vertical eigenfunctions. These two characteristic equations are compared with previous results in the literature. Although the two derivations lead to dramatically different forms for the characteristic equation, we prove that they are equivalent. The most important observation is the discovery of an internal $1:1$ resonance both in the shallow water model and the fully two-dimensional finite depth model, where symmetric fluid modes are coupled to the vessel motion. Numerical evaluation of the resonant and nonresonant modes are presented. The implications of the resonance for the fluid dynamics, and for the nonlinear coupled dynamics near the resonance are also discussed.

— April 25, 2012—

Contents

1 Introduction

In Cooker's sloshing experiment [9], a rectangular vessel containing fluid is suspended from a stationary beam by two cables which are free to rotate in a vertical plane. A schematic of the experiment is shown in Figure 1. The rectangular vessel has length L, height d, and unit width, and is partially filled with fluid of mean depth h_0. The tank is suspended by two rigid cables of equal length ℓ, and the cables make an angle θ with the vertical. The base of the tank remains horizontal during the motion.

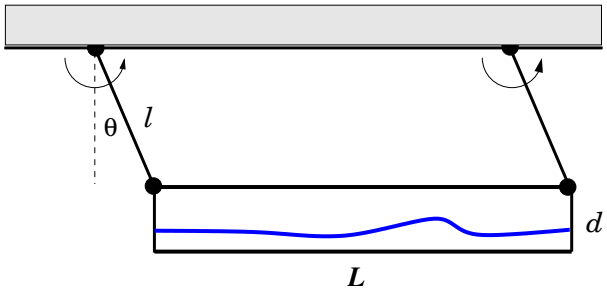

Figure 1: Schematic of Cooker's experimental configuration [9].

It is an experiment in the spirit of Taylor [23]: it is simple, easy to construct, robust and illuminates a fundamental question in fluid mechanics. In this case the question is the effect of vehicle coupling on fluid sloshing. Indeed, it is one of the simplest configurations that allows precise study of the coupled dynamics between the fluid motion and the vessel motion. The problem of sloshing in stationary vessels is already a very difficult problem to study both experimentally and theoretically (cf. Ibrahim [16] and Faltinsen & Timokha [10] and references therein). The coupled dynamics between fluid sloshing and vessel motion brings in a new dimension and the potential for enhancing or diminishing the sloshing motion through vehicle dynamics. The coupled problem is of great practical interest in the transport of liquids along roads, maritime fluid transport, and industrial applications. Hence a prototype for understanding the fundamentals of coupling is of great interest.

Cooker developed a linear theory of the coupled problem with a shallow-water model for the fluid. The theory showed that the coupling changed the set of natural frequencies, and the theory showed very good agreement with experimental results. Cooker's theory was extended by Alemi Ardakani & Bridges [3] to include a nonlinear shallow water model for the fluid, but the vessel model was still linear. A numerical algorithm for simulation of the coupled problem was developed with careful attention taken to the maintenance of the overall energy conservation and energy partition between fluid and vessel.

A related problem is that of *tuned liquid dampers* or *tuned sloshing dampers* considered by Ikeda & Nakagawa [17] and Frandsen [11]. A schematic is shown in Figure 2. For definiteness call these systems TLDs. A TLD consists of a vessel containing fluid, but constrained to move in the horizontal direction only, with the vessel motion governed by a linear spring-mass-damper model, and may include a horizontal forcing function. The nonlinear characteristics of TLDs are very different from Cooker's experiment, but at the linear level the two systems are equivalent. Neglecting damping and forcing, and taking

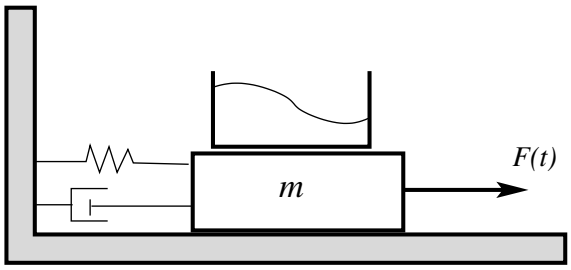

Figure 2: Schematic of a TLD system following Figure 1 of [11].

the fluid to be irrotational, the governing equations are exactly equivalent to the linearized equations governing Cooker's experiment. This equivalence is shown in §3.1. However the nonlinear equations are very different since the vessel motion in Cooker's experiment is fully nonlinear, governed by a forced pendulum equation (see equation (1.1) below), and includes vertical as well as horizontal motion.

Experiments for the case where the spring constant is zero have recently been reported by Herczyński & Weidman [15]. Spring constant zero corresponds to Cooker's experiment in the limit as the suspension length goes to infinity. These experiments are quite difficult because there is no restoring force and so the vessel may drift in addition to harmonic motion. Using a special low-friction cart, and carefully-controlled initial conditions, the experiments showed excellent agreement with the theory. However, without the spring force a 1:1 resonance, which is of great interest here, can not occur.

Ikeda & Nakagawa [17] used a modal expansion to study the nonlinear problem for TLDs. They included one anti-symmetric fluid mode, one symmetric fluid mode and the vessel mode, resulting in a $6-$dimensional system of nonlinear ODES. Their linear analysis is reviewed in §4. An infinite modal expansion for the linear TLD problem was first given by Frandsen [11]. The *linearized* TLD model in [11] is exactly equivalent to the *linearized* model for Cooker's experiment (cf. §3.1). The linear model and results of Frandsen [11] can be interpreted as the first reported results on the natural frequencies of a linear finite-depth model for Cooker's experiment. A cosine expansion is used and infinite-product representation for the characteristic equation is presented, and numerical simulations of the nonlinear problem are presented. A key assumption in [11] is that symmetric modes are neglected since they exert no horizontal force on the vessel. We extend Frandsen's analysis by giving a new explicit sum representation for the characteristic equation and show moreover that the symmetric modes can be important when they couple to the vessel motion at resonance.

Independently, Yu [25] extended Cooker's model to include a fully two-dimensional model for the fluid, but restricted to linear fluid motion and linear vessel motion. Implicitly, an expansion in terms of "vertical eigenfunctions" [18] was used but the characteristic equation gives the same results as [11]. A range of results on the effect of fluid depth and mass ratio on the first mode were presented, showing a dramatic effect of finite but non-shallow depth.

The cosine expansion has as its organizing centre the cosine-eigenfunctions in the horizontal direction ($x-$direction) and the vertical eigenfunction expansion has as its organizing centre a class of eigenfunctions in the vertical direction ($y-$direction). The two representations of the solution are very different. However, we prove, by constructing

an explicit transformation, that the two representations are exactly equal. With this transformation we are able to show that the results of Frandsen [11] and Yu [25] are equivalent.

In previous work (e.g. [9, 17, 11, 25, 3]) there was some mystery about a "resonance". Cooker noted a curious resonance, where the second mode of the coupled problem resonated with the natural frequency of the dry vessel, but the resonance did not satisfy the characteristic equation. Frandsen [11] acknowledges that a resonance exists, but only considers the asymptotic case of small mass ratio (where the vessel mass is much greater than the fluid mass). Yu [25] disputed the role of resonance noting that there is no mechanism for continued energy input (see §3.5 of [25]).

In this paper the theory of Cooker's experiment in particular, and the theory of resonance in dynamic coupling in general, are extended in three directions. First, for the case of Cooker's experiment, a fully nonlinear model for the vessel motion is derived. It turns out to be a forced pendulum equation, with the forcing determined by the fluid pressure $p(x, y, t)$ on the vessel walls

$$\ddot{\theta} + \frac{g}{\ell}\sin\theta = \frac{1}{m_v \ell}\int_0^L \int_0^{h(x,t)} (p_x \cos\theta + p_y \sin\theta)\,\mathrm{d}y\mathrm{d}x\,, \tag{1.1}$$

where $y = h(x, t)$ is the position of the fluid free surface in the vessel, and g is the gravitational constant. Secondly, the coupled fluid-vessel equations for Cooker's experiment are linearized and a new derivation of the coupled characteristic equation is given. The cosine expansion approach is compared with the vertical eigenfunction approach and shown to be equivalent. Thirdly, we have discovered that there is a resonance, where the uncoupled symmetric fluid mode resonates exactly with an anti-symmetric fluid mode joined with the vessel motion. It is an *internal resonance*, where two natural frequencies are equal and have linearly independent eigenvectors. In the Hamiltonian systems literature it is called a $1:1$ resonance, or sometimes the $1:1$ semisimple resonance (e.g. [13]). This resonance was implicit in the shallow water analysis in [9] and here we give an explicit proof of the existence of the resonance in the shallow water model and then extend it to the finite depth model.

Cooker [9] showed that the natural frequencies in shallow water, for dynamic coupling between the vessel motion and an anti-symmetric fluid mode, are determined by the roots of $\mathrm{D}^{\mathrm{SW}}(s) = 0$ where

$$\mathrm{D}^{\mathrm{SW}}(s) = \frac{G}{s} - Rs - \tan s\,, \tag{1.2}$$

where s is the dimensionless natural frequency

$$s = \frac{\omega}{\sqrt{gh_0}}\frac{L}{2}\,, \tag{1.3}$$

and ω is the dimensional natural frequency. The dimensionless parameters G and R were first introduced in [9] and they are defined by

$$R = \frac{m_v}{m_f}\,, \quad G = \frac{\nu L^2}{4gh_0 m_f} \quad \text{with} \quad \nu = \frac{g}{\ell}(m_v + m_f)\,, \tag{1.4}$$

where m_v is the mass of the dry vessel, and $m_f = \rho h_0 L$ is the mass of the fluid per unit width. The parameter ν is the spring stiffness parameter due to the gravitational restoring force.

The characteristic function (1.2) can not have a $1:1$ resonance since all the roots are simple. To identify the resonance, we show that there is a missing term in (1.2). The characteristic equation should be the product of two terms

$$\Delta^{\mathrm{SW}}(s) = \mathrm{P}^{\mathrm{SW}}(s)\,\mathrm{D}^{\mathrm{SW}}(s) \quad \text{with} \quad \mathrm{P}^{\mathrm{SW}}(s) = \sin(s)\,. \tag{1.5}$$

With the additional term there is an explicit $1:1$ resonance when both factors vanish simultaneously. This occurs precisely when G and R satisfy

$$G = s_m^2\,R\,, \quad \text{with } s_m = m\pi \text{ for any } m \in \mathbb{N}\,. \tag{1.6}$$

This observation makes explicit the resonance noted in [9].

We show in general that the characteristic function in all cases (the shallow water model [9, 3], the finite modal expansion [17], the cosine expansion [11], and the vertical eigenfunction expansion [25]) is the product of two functions

$$\Delta(s) = \mathrm{P}(s)\,\mathrm{D}(s)\,, \tag{1.7}$$

where s is the dimensionless frequency (1.3) in all cases. The roots of $\mathrm{D}(s) = 0$ are the modes which couple an anti-symmetric fluid mode with the vessel mode, and the roots of $\mathrm{P}(s) = 0$ are associated with the symmetric fluid modes.

The product structure of the characteristic equation (1.7) arises because the eigenvalue problem for the natural frequency has a block diagonal structure. An important consequence of this structure is that the eigenfunctions associated with the roots of $\mathrm{P} = 0$ are always linearly independent from the eigenfunctions associated with the roots of $\mathrm{D} = 0$. The product structure (1.7) has three principal solutions:

1. $\mathrm{D}(s) = 0$ but $\mathrm{D}'(s) \neq 0$ and $\mathrm{P}(s) \neq 0$: anti-symmetric fluid mode coupled to vessel motion.

2. $\mathrm{P}(s) = 0$ but $\mathrm{P}'(s) \neq 0$ and $\mathrm{D}(s) \neq 0$: symmetric fluid mode decoupled from vessel motion.

3. $\mathrm{D}(s) = 0$ and $\mathrm{P}(s) = 0$ but $\mathrm{D}'(s) \neq 0$ and $\mathrm{P}'(s) \neq 0$: internal $1:1$ resonance with a symmetric and anti-symmetric fluid mode coupled to the vessel motion.

The third condition is equivalent to $\Delta(s) = \Delta'(s) = 0$ which is the necessary condition for a $1:1$ resonance. The second class of solutions are symmetric modes which do not generate any coupling with the vessel motion. Figure 3 shows the first two mode shapes for the free oscillations of the fluid, and it apparent why the symmetric mode can generate free oscillations without affecting the vessel motion. The pressure is symmetric and so the force on the right vessel wall exactly balances that on the left.

It is important to emphasize that the resonance here is an *internal resonance* between normal modes: two linearly independent eigenfunctions corresponding to the same natural frequency. There is no forcing present. The theory of resonance due to external forcing requires different methods (e.g. Ockendon et al. [20, 21], Chapter 2 of [16]). Adding external forcing to an internal resonance would greatly enhance the range of response but external forcing is not considered in this paper. The internal resonances are of interest for two reasons: at the linear level it is a mechanism for excitation of symmetric fluid mode

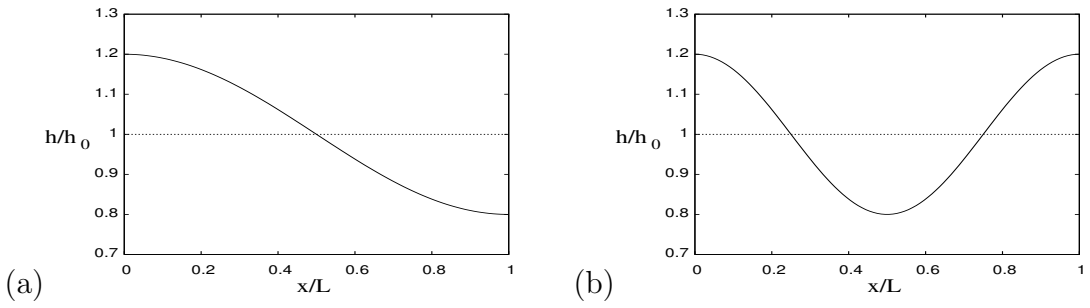

Figure 3: Mode shapes for the (a) first anti-symmetric and (b) first symmetric free oscillation modes

coupling to the vessel motion, and at the nonlinear level a $1:1$ resonance can give rise to much more dramatic fluid-vessel motion. A $1:1$ resonance in a different physical setting (Faraday experiment) is analyzed by [12, 13] and it gives some idea of the dramatic effect of the $1:1$ resonance in the weakly nonlinear problem. The effect of nonlinearity on the resonance is not considered in this paper (some comments on nonlinearity are in §10).

There are other potential internal resonances as well. For example the roots of either $\mathrm{P}(s)=0$ or $\mathrm{D}(s)=0$ may have modes with integer ratio, the most common of which is the $1:2$ resonance. For example in the case of free oscillations of the sloshing problem – with surface tension – it is shown by Vanden-Broeck [24] that a $1:2$ resonance occurs. A generalization of that $1:2$ resonance may also occur in modified form in the coupled problem if surface tension is added to the fluid. There is also the potential for rational ratios of any order: that is solutions of the form

$$\Delta(ms)=\Delta(ns)=0 \quad \text{for some natural numbers } (m,n)\,.$$

These higher-order resonances are not considered in this paper.

In this paper we extend all three classes of solutions identified above to the finite-depth model. When the depth is not small, the characteristic equation is much more complicated and will also depend on a third parameter: the depth ratio

$$\delta=\frac{h_0}{L}\,. \tag{1.8}$$

In this paper a new derivation of the coupled characteristic equation for finite depth is presented, using both the cosine expansion as in [11] and the vertical eigenfunction expansion as in [18, 25]. We find that the generalization of the shallow water resonance condition (1.6) is

$$\frac{G}{s_m}=Rs_m+s_m\sum_{n=1}^{\infty}\frac{c_n^2}{\frac{1}{2}k_nL}\tanh(\tfrac{1}{2}k_nL)\,. \tag{1.9}$$

with

$$s_m=m\pi\sqrt{\frac{\tanh(2m\pi\delta)}{2m\pi\delta}}\,,\quad \text{for any } m\in\mathbb{N}\,. \tag{1.10}$$

In the finite depth case, the range of physically-realizable values of parameters for the $1:1$ resonance is greatly extended. Both (1.6) and (1.9) are straight lines in the $(R,G)-$plane for each fixed m, but the slope for (1.6) is quite large whereas the slope decreases with

increasing δ and becomes horizontal, and the $G-$intercept decreases, in the limit $\delta \to \infty$. Graphs illustrating the $\delta-$dependence of the resonance lines are presented in §9.3.

An outline of the paper is as follows. In §2 a sketch of the derivation of the new characteristic equation for shallow water (1.5) is presented with details given in Appendix A. The derivation of the new fully nonlinear model for Cooker's experiment is given in Appendix B. The fluid motion is governed by Euler's equation relative to a moving frame, and the nonlinear equation governing the vessel motion is obtained from a variational principle, leading to (1.1). The nonlinear equations with the fluid assumed to be irrotational are also derived in Appendix B.2.

With the derivations of the equations in Appendix B, the body of the paper for the finite depth analysis starts with the linearization of the governing equations in §3. The linear equations are derived and then solutions which are harmonic are considered. The remainder of the paper is then the study of the time-harmonic solutions in order to determine the natural frequencies of the coupled problem. Section 5 presents the details of the cosine expansion approach to determining the characteristic equation and §6 presents the details using the vertical eigenfunction expansion. The explicit proof that the two representations are equivalent is given in §7.

The derivation of the $1:1$ resonance and its implications for the linear problem are presented in §9. Numerical results for the non-resonant characteristic equation are presented in §8 and for the resonant case in §9.3. In the concluding remarks §10 some speculation on the implications of the $1:1$ resonance for the nonlinear problem is given.

2 1:1 resonance in the shallow water limit

The characteristic equation in shallow water (1.2) does not have a $1:1$ resonance. A necessary condition for a $1:1$ resonance is that there exist a value of s satisfying

$$\mathrm{D}^{\mathrm{SW}}(s) = \frac{d}{ds}\mathrm{D}^{\mathrm{SW}}(s) = 0\,.$$

A calculation shows that all the roots of $\mathrm{D}^{\mathrm{SW}}(s) = 0$ are simple. However, with a minor change in the derivation of the characteristic equation, we can show that there is an additional term. Start with the linear shallow water equations in [9]

$$\begin{aligned} h_t + h_0 u_x &= 0 \\ u_t + g h_x &= -\ddot{q} \\ m_v \ddot{q} + \nu q &= \rho g h_0 (h(L,t) - h(0,t))\,, \end{aligned} \tag{2.1}$$

with boundary conditions $u(0,t) = u(L,t) = 0$. Here $q(t) = \ell\theta(t)$. By considering solutions that are periodic in time of frequency ω, it is shown in Appendix A that the complete characteristic equation is given by (1.5). The addition of the factor $\sin(s)$ in (1.5) makes the $1:1$ internal resonance explicit. The resonance condition is

$$\Delta^{\mathrm{SW}}(s) = \frac{d}{ds}\Delta^{\mathrm{SW}}(s) = 0\,,$$

or

$$\sin(s)\left(\frac{G}{s} - Rs - \tan(s)\right) = 0$$

and

$$\cos(s)\left(\frac{G}{s}-Rs-\tan(s)\right)+\sin(s)\left(-\frac{G}{s^2}-R-1-\tan^2(s)\right)=0\,.$$

There are no double roots with $\sin(s)\neq 0$. Hence the only possible double root corresponds to $\sin(s)=0$ giving $s=m\pi$ and $\cos(s)=(-1)^m$ and the second condition reduces to $G=m^2\pi^2R$ confirming (1.6). The condition $G=m^2\pi^2R$ is precisely the condition for resonance in §3.4 of [9]. In terms of physical parameters the resonance condition is

$$1+\frac{m_f}{m_v}=4m^2\pi^2\frac{\ell}{L}\frac{h_0}{L}\,. \tag{2.2}$$

Although experiments at resonance were not reported in [9], a check of the parameter values in the experiments of [9] shows that the resonances condition (2.2) is physically achievable for at least $m=1$ and $m=2$,

At resonance the vessel natural frequency equals one of the *symmetric* free modes of the fluid oscillation

$$\omega^v:=\frac{\nu}{m_v}=2m\frac{\pi}{L}\sqrt{gh_0}:=\omega_m\,,\quad \text{for some } m\,. \tag{2.3}$$

The symmetric fluid modes exert no horizontal force on the vessel. However, at resonance, these symmetric modes can mix with the vessel motion. There is a continuum of such solutions in the linear problem, with eigenfunctions

$$\begin{aligned} u_m(x,t) &= 2\sqrt{gh_0}\sin(\tfrac{1}{2}m\kappa x)\left[\tfrac{A_m}{\sqrt{gh_0}}\cos(\tfrac{1}{2}m\kappa x)+m\kappa\sin(\tfrac{1}{2}m\kappa x)\widehat{q}_m\right]\sin(\omega_m t)\,,\\ h_m(x,t) &= \left[\tfrac{A_m h_0}{\sqrt{gh_0}}\cos(m\kappa x)+m\kappa h_0\widehat{q}_m\sin(m\kappa x)\right]\cos(\omega_m t)\,,\\ q_m(t) &= \widehat{q}_m\cos(\omega_m t)\,. \end{aligned} \tag{2.4}$$

In these expressions, A_m and $\widehat{q}_m$ are arbitrary real numbers, and $\kappa:=2\pi/L$.

In the case of shallow water the $1:1$ resonance (2.3) is much more severe than in finite depth. This severity is due to the fact that the fluid natural frequencies have an infinite order resonance: $\omega_m=m\omega_1$. Hence an infinite number of symmetric fluid modes resonate with the vessel mode at the resonance (2.3). However, this degeneracy disappears when the depth is finite leaving a pure $1:1$ resonance.

3 Linear dynamically-coupled equations

Suppose henceforth that the shallow water approximation is not operational. The fully-nonlinear equations for the fluid motion with arbitrary finite depth coupled to vessel motion are derived in Appendix B. The main new result is that the vessel motion is governed by the nonlinear pendulum equation forced by the fluid motion (1.1).

The starting point for the linear analysis of the coupled problem, with the fluid taken to be irrotational, is obtained by linearizing the boundary conditions (B-13)-(B-14), (B-15)-(B-16), and the vehicle equation (B-17).

To leading order, the vessel position coordinates $(q_1(t),q_2(t))$ in (B-3) are approximated by $\dot{q}_1\approx\ell\dot{\theta}$ and $\dot{q}_2\approx 0$. The governing equation for ϕ in the linear approximation is still Laplace's equation

$$\phi_{xx}+\phi_{yy}=0\,,\quad 0<y<h_0\,,\quad 0<x<L\,, \tag{3.1}$$

and the bottom and sidewall boundary conditions simplify to

$$\begin{aligned} \phi_y &= 0 \quad \text{at} \quad y = 0\,, \\ \phi_x &= \ell\dot{\theta} \quad \text{at} \quad x = 0 \text{ and } x = L\,, \\ \phi_y &= h_t \quad \text{and} \quad \phi_t + gh = 0 \quad \Rightarrow \quad \phi_{tt} + g\phi_y = 0\,, \quad \text{at } y = h_0\,. \end{aligned} \tag{3.2}$$

The linearized vessel equation is

$$\frac{d}{dt}\left[\int_0^L \int_0^{h_0} \rho\phi_x \,\mathrm{d}y\mathrm{d}x + m_v\ell\dot{\theta}\right] + g(m_v + m_f)\theta = 0\,. \tag{3.3}$$

3.1 Comparison with Frandsen's TLD model

To show that the linear equations (3.1)-(3.2) are equivalent to Frandsen's linearized TLD model, let

$$\phi(x, y, t) = \ell\dot{\theta}\, x + \Phi(x, y, t)\,,$$

and define

$$X(t) = \ell\theta(t)\,.$$

Then substitution into (3.1)-(3.2) gives a boundary value problem for $\Phi(x, y, t)$,

$$\Phi_{xx} + \Phi_{yy} = 0\,, \quad 0 < y < h_0\,, \quad 0 < x < L\,, \tag{3.4}$$

with boundary conditions

$$\begin{aligned} \Phi_y &= 0 \quad \text{at} \quad y = 0 \\ \Phi_x &= 0 \quad \text{at} \quad x = 0, L\,, \\ g\Phi_y &= -\Phi_{tt} - x\dddot{X} \quad \text{at} \quad y = h_0\,. \end{aligned} \tag{3.5}$$

The linearized vessel equation is

$$(m_v + m_f)\ddot{X} + \nu X = -\int_0^L \int_0^{h_0} \rho\Phi_{xt} \,\mathrm{d}y\mathrm{d}x = \int_0^{h_0} \rho\Phi_t \,\mathrm{d}y\Big|_{x=L}^{x=0}\,, \tag{3.6}$$

with $\nu = \frac{g}{\ell}(m_v + m_f)$. These equations for Φ are precisely equations (2.6) for ϕ on page 312 of [11], with the appropriate change of notation, and setting the damping coefficient c and the forcing function $F(t)$ to zero in [11]. In summary, the linear equations for the TLD model are exactly equivalent to the linearized equations for Cooker's sloshing experiment. However, the nonlinear equations for the two systems are different.

3.2 Natural frequencies of the linear coupled problem

To determine the natural frequencies of the linearized coupled problem, express ϕ, h and θ as time-periodic functions with frequency ω,

$$\phi = \widehat{\phi}\cos\omega t\,, \quad h = \widehat{h}\,\sin\omega t\,, \quad \theta = \widehat{\theta}\,\sin\omega t\,. \tag{3.7}$$

Then

$$\widehat{h} = \frac{\omega}{g}\widehat{\phi}\Big|^{y=h_0}\,, \tag{3.8}$$

and $\widehat{\phi}$ and $\widehat{\theta}$ satisfy the boundary value problem

$$\widehat{\phi}_{xx} + \widehat{\phi}_{yy} = 0\,, \quad 0 < y < h_0\,, \quad 0 < x < L\,, \tag{3.9}$$

with boundary conditions

$$\begin{aligned} \widehat{\phi}_y &= 0 \quad \text{at} \quad y = 0\,, \\ \widehat{\phi}_y &= \tfrac{\omega^2}{g}\widehat{\phi} \quad \text{at} \quad y = h_0\,, \\ \widehat{\phi}_x &= \ell\omega\widehat{\theta} \quad \text{at} \quad x = 0, L\,, \end{aligned} \tag{3.10}$$

and vessel equation

$$\left(\frac{g(m_v + m_f)}{\omega} - m_v\ell\omega\right)\widehat{\theta} = \int_0^L \int_0^{h_0} \rho\widehat{\phi}_x \,\mathrm{d}y\mathrm{d}x\,. \tag{3.11}$$

The coupled equations (3.9)-(3.11) form an eigenvalue problem for the natural frequency ω of the coupled problem. The equation (3.9) with the boundary conditions (3.10) is well studied in the case where $\theta(t)$ is given – the forced problem (see §2.2.2 of [18] and §2.6 of [16]). In the coupled problem, an additional equation (3.11) is included for the vessel motion.

4 Method 1: finite modal expansion

The first approach proposed for the coupled linear finite depth problem (3.1)-(3.3) was a finite modal expansion by Ikeda & Nakagawa [17]. They expressed the fluid motion in terms of the first anti-symmetric and first symmetric fluid mode, coupled to the vessel motion (see equation (15) in [17]). Their motivation was to study the nonlinear problem by modelling it with 3 coupled nonlinear ODEs. However, for the purposes of this paper we review the linear version of their modal expansion as it provides a simplified model of the full infinite expansion considered in §5, and has the three principal solutions in simplified form.

Consider the three term approximation

$$\phi(x,y,t) = \dot{X}(t)\left(x - \tfrac{1}{2}L\right) + a_0(t)\frac{\cosh(\alpha_0 y)}{\cosh(\alpha_0 h_0)}\cos(\alpha_0 x) + b_1(t)\frac{\cosh(\beta_1 y)}{\cosh(\beta_1 h_0)}\cos(\beta_1 x)\,, \tag{4.1}$$

where $X(t) = \ell\theta(t)$, $\alpha_0 = \pi/L$ and $\beta_1 = 2\pi/L$. It satisfies Laplace's equation. Substitution into the boundary conditions (3.2)-(3.3) gives the three coupled equations

$$\begin{aligned} \ddot{b}_1 + g\beta_1 \tanh(\beta_1 h_0)\, b_1 &= 0 \\ \ddot{a}_0 + g\alpha_0 \tanh(\alpha_0 h_0)\, a_0 &= \frac{4}{L\alpha_0^2}\dddot{X} \\ (m_v + m_f)\ddot{X} + \nu X &= \frac{2\rho}{\alpha_0}\tanh(\alpha_0 h_0)\,\dot{a}_0\,. \end{aligned} \tag{4.2}$$

With appropriate change of notation, these are the linear parts of equations (18a)-(18e) in [17]. The second and third equations are equivalent to equations (20)-(21) in [17].

The notation (a_1, a_2, x_1) there corresponds to (a_0, b_1, X) here. The first equation in (4.2) is dropped from the linear analysis in [17], since it represents the symmetric mode and decouples from the anti-symmetric mode and the vehicle mode. All three modes are retained here.

The harmonic approximation,

$$X(t) = \widehat{X}\,\sin(\omega t)\,, \quad a_0(t) = \widehat{a_0}\,\cos(\omega t) \quad \text{and} \quad b_1(t) = \widehat{b_1}\,\cos(\omega t)\,,$$

reduces the ODEs to a homogeneous matrix equation

$$\begin{bmatrix} -\omega^2 + g\beta_1 \tanh(\beta_1 h_0) & 0 & 0 \\ 0 & -\omega^2 + g\alpha_0 \tanh(\alpha_0 h_0) & \frac{4}{L\alpha_0^2}\omega^3 \\ 0 & \frac{2\rho}{\alpha_0}\omega \tanh(\alpha_0 h_0) & -(m_v + m_f)\omega^2 + \nu \end{bmatrix} \begin{pmatrix} \widehat{b_1} \\ \widehat{a_0} \\ \widehat{X} \end{pmatrix} = \begin{pmatrix} 0 \\ 0 \\ 0 \end{pmatrix}. \tag{4.3}$$

Vanishing of the determinant of the coefficient matrix then gives the characteristic equation $\Delta^{\rm IN}(\omega) = 0$ with

$$\Delta^{\rm IN}(\omega) = {\rm P}^{\rm IN}(\omega){\rm D}^{\rm IN}(\omega)\,, \tag{4.4}$$

where

$${\rm P}^{\rm IN}(\omega) = -\omega^2 + g\beta_1 \tanh(\beta_1 h_0)\,, \tag{4.5}$$

and

$${\rm D}^{\rm IN}(\omega) = \big(-\omega^2 + g\alpha_0 \tanh(\alpha_0 h_0)\big)\big(-(m_v + m_f)\omega^2 + \nu\big) - \frac{8\rho}{L\alpha_0^3}\omega^4\omega \tanh(\alpha_0 h_0)\,. \tag{4.6}$$

The decoupling of the b_1 mode is reflected in the block diagonal structure of the coefficient matrix in (4.3). As a consequence, the eigenvector associated with the b_1 mode is linearly independent from any of the eigenvectors of the other modes. A fact which is important for the internal $1:1$ resonance. The three principal solutions are:

1. ${\rm D}^{\rm IN}(\omega) = 0$ and ${\rm P}^{\rm IN}(\omega) \neq 0$: anti-symmetric fluid mode coupled to vessel
2. ${\rm P}^{\rm IN}(\omega) = 0$ and ${\rm D}^{\rm IN}(\omega) \neq 0$: symmetric fluid mode decoupled from vessel motion
3. ${\rm D}^{\rm IN}(\omega) = 0$ and ${\rm P}^{\rm IN}(\omega) = 0$: internal $1:1$ resonance with solutions 1 & 2 coupled.

The first principal solution is the one considered in [17]: see equation (23) in [17] where the two roots of ${\rm D}^{\rm IN}(\omega) = 0$ are labelled q_1^2 and q_2^2. The second class of solutions has $a_1 = 0$ and $X = 0$ but $b_1 \neq 0$: it is a symmetric free oscillation.

Since the third class of solutions requires both functions to vanish it puts a constraint on parameter space. For comparison with other methods in this paper first put the factors in (4.4) into dimensionless form using (1.3) and (1.4),

$$\begin{aligned} {\rm P}^{\rm IN}(s) &= -s^2 + \pi^2 \frac{\tanh(\beta_1 h_0)}{\beta_1 h_0} \\ {\rm D}^{\rm IN}(s) &= \big[-s^2 + (\tfrac{1}{2}\alpha_0 L)^2 \mathcal{T}_0\big]\big[G - (1+R)s^2\big] - \frac{8\mathcal{T}_0}{(\alpha_0 L)^2}s^4\,, \end{aligned} \tag{4.7}$$

with

$$\mathcal{T}_0 := \frac{\tanh(\alpha_0 h_0)}{\alpha_0 h_0}\,. \tag{4.8}$$

Now substitute the solution of $\mathrm{P}^{\mathrm{IN}}(s) = 0$,

$$s_0 = \pi\sqrt{\frac{\tanh(\beta_1 h_0)}{\beta_1 h_0}}\,, \tag{4.9}$$

into $\mathrm{D}^{\mathrm{IN}}(s) = 0$ giving, after some rearrangement,

$$\frac{G}{s_0} - Rs_0 = s_0 + \frac{8\mathcal{T}_0}{(\alpha_0 L)^2}\frac{s_0^3}{(\frac{1}{2}\alpha_0 L)^2\mathcal{T}_0 - s_0^2}\,. \tag{4.10}$$

This condition is the analogue of the condition (1.6) for the shallow water model and the analogue of the condition (1.9) for the finite-depth model. It gives a $\delta-$dependent straight line in the $(R, G)-$plane by noting that $\alpha_0 h_0 = L\alpha_0\delta$ in dimensionless form.

To compare with (1.6) take the limit $\delta \to 0$ giving $\mathcal{T}_0 = 1$ and $s_0 = \pi$ and so

$$G = \pi^2 R + \pi^2 - \frac{32}{3}\,, \tag{4.11}$$

which has the same slope as the line in (1.6) but with a slightly lower value of the $G-$intercept.

For finite δ, it is not obvious that (4.10) is related to the exact finite depth condition (1.9). However, it is related, and the relationship between the two is easier to see once the infinite cosine expansion is introduced and is therefore considered in §5.

The resonance (4.10) is not considered in [17]. However, they consider two other forms of resonance. The first resonance considered in [17] is a resonance between the dry vessel ($\sqrt{k/Q_{17}}$ in the notation there) and the *first anti-symmetric mode* (see discussion in the beginning of §3 on page 31 of [17]). They also bring in a second form of resonance by introducing a forcing function, and then a resonance can be introduced by choosing the forcing frequency near one of the system frequencies. The principal aim in [17] is the effect of nonlinearity on these resonances.

5 Method 2: an infinite cosine expansion

In the absence the coupling equation the linear problem (3.9)-(3.10) is equivalent to the problem of forced oscillations with $\theta(t)$ specified. This problem was first considered by Graham & Rodriguez [14] (see also §2.6.1 of [16] and §5.2 of [10]). Their strategy for solving (3.9)-(3.10) is to transform $\widehat{\phi}$ so that the inhomogeneous boundary conditions at $x = 0, L$ are moved to $y = h_0$. Then a cosine expansion in the $x-$direction can be used. Let

$$\widehat{\phi}(x, y) = \ell\omega\widehat{\theta}\left(x - \tfrac{1}{2}L\right) + \widehat{\Phi}(x, y)\,. \tag{5.1}$$

The function $\widehat{\Phi}(x, y)$ then satisfies Laplace's equation and the following boundary conditions

$$\widehat{\Phi}_y = \frac{\omega^2}{g}\widehat{\Phi} + \ell\widehat{\theta}\frac{\omega^3}{g}\left(x - \tfrac{1}{2}L\right)\,, \quad y = h_0\,, \tag{5.2}$$

$$\widehat{\Phi}_y = 0\,, \quad y = 0\,, \tag{5.3}$$

$$\widehat{\Phi}_x = 0\,, \quad x = 0, L\,. \tag{5.4}$$

The inhomogeneous term at $y = h_0$ has the following cosine expansion

$$x - \frac{L}{2} = \sum_{n=0}^{\infty} p_n \cos(\alpha_n x) = -\frac{4}{L} \sum_{n=0}^{\infty} \frac{1}{\alpha_n^2} \cos(\alpha_n x)\,, \quad \alpha_n = (2n+1)\frac{\pi}{L}\,. \tag{5.5}$$

This form of the boundary condition suggests that the following form for the $\widehat{\Phi}$ solution

$$\widehat{\Phi}(x,y) = \sum_{n=1}^{\infty} b_n \frac{\cosh(\beta_n y)}{\cosh(\beta_n h_0)} \cos(\beta_n x) + \sum_{n=0}^{\infty} a_n \frac{\cosh(\alpha_n y)}{\cosh(\alpha_n h_0)} \cos(\alpha_n x)\,, \tag{5.6}$$

where $\beta_n = 2n\pi/L$. The first term gives the homogeneous solution and the second term gives the particular solution associated with the $\widehat{\theta}$ term in (5.2). The coefficients a_n and b_n are determined by substitution into the boundary condition at $y = h_0$, giving

$$\left(\beta_n \tanh(\beta_n h_0) - \frac{\omega^2}{g}\right) b_n = 0\,, \tag{5.7}$$

and

$$\left(\alpha_n \tanh(\alpha_n h_0) - \frac{\omega^2}{g}\right) a_n = -\ell\omega\widehat{\theta}\, \frac{4}{L\alpha_n^2} \frac{\omega^2}{g}\,. \tag{5.8}$$

This completes the solution of the forced problem. Now substitute the general form for $\widehat{\phi}(x,y)$ in (5.1) into the coupling equation for $\widehat{\theta}$,

$$(m_v + m_f)\left(\frac{g}{\omega} - \ell\omega\right)\widehat{\theta} = \int_0^L \int_0^{h_0} \rho\widehat{\Phi}_x \,\mathrm{d}y\mathrm{d}x\,,$$

or

$$(m_v + m_f)\left(\frac{g}{\omega} - \ell\omega\right)\widehat{\theta} = -2\rho \sum_{n=0}^{\infty} \frac{a_n}{\alpha_n} \tanh(\alpha_n h_0)\,. \tag{5.9}$$

The three equations (5.7)-(5.9) are three homogeneous equations for the unknowns $\widehat{\theta}$, $a_0, a_1, \ldots,$ and $b_1, b_2, \cdots$. The first equation (5.7) is homogeneous, diagonal and decouples from the other equations. Its characteristic function is

$$\mathrm{P}^{\cos}(\omega) = \prod_{m=1}^{\infty} \left(\omega^2 - g\beta_m \tanh(\beta_m h_0)\right). \tag{5.10}$$

The full characteristic equation is $\Delta^{\cos}(\omega) = 0$ with

$$\Delta^{\cos}(\omega) = \mathrm{P}^{\cos}(\omega)\mathrm{D}^{\cos}(\omega)\,. \tag{5.11}$$

The symmetric modes, satisfying $\mathrm{P}^{\cos}(\omega) = 0$, do not appear in the coupling equation (5.9). The $1:1$ resonance of the system is considered in §9.

In the remainder of this section the characteristic function, $\mathrm{D}^{\cos}(\omega)$, for non-resonant *strictly coupled* dynamics is derived. It is this characteristic equation which was first studied in [11].

Set $b_n = 0$ for all n and assume $\widehat{\theta} \neq 0$. Then (5.8) can be solved for a_n and substituted into (5.6)

$$\widehat{\Phi}(x,y) = -\ell\omega\widehat{\theta}\, \frac{4\omega^2}{Lg} \sum_{n=0}^{\infty} \frac{(\alpha_n \tanh(\alpha_n h_0) - \omega^2/g)^{-1}}{\alpha_n^2} \frac{\cosh(\alpha_n y)}{\cosh(\alpha_n h_0)} \cos(\alpha_n x)\,. \tag{5.12}$$

Substitution into the coupling equation (5.9) then gives $\mathrm{D}^{\cos}(\omega) = 0$ with

$$\mathrm{D}^{\cos}(\omega) = \left[(m_v + m_f)\left(\frac{g}{\omega} - \ell\omega\right) - \frac{8\ell m_f}{L^2 h_0}\frac{\omega^3}{g}\sum_{n=0}^{\infty}\frac{1}{\alpha_n^3}\frac{\tanh(\alpha_n h_0)}{\left(\alpha_n \tanh(\alpha_n h_0) - \frac{\omega^2}{g}\right)}\right]. \quad (5.13)$$

This characteristic equation is implicit in [11]. The strategy there is to use an infinite determinant expansion resulting in a product formula (see equation (4.1) in [11]), which is then analyzed in the limit $R \to \infty$, with R defined in (1.4).

Here the explicit form (5.13) will be used. Exact solutions are still impossible, but the explicit form is useful for numerical computation of the frequencies. First transform (5.13) to dimensionless form. Let

$$\gamma_n = (2n+1)\pi \quad \text{and} \quad T_n = \tanh(\alpha_n h_0) = \tanh(\gamma_n \delta)\,.$$

Then, using the Cooker parameters (1.4), dividing by $\omega m_f L$, noting that

$$\frac{\ell}{L} = \frac{1}{4\delta}\frac{(1+R)}{G}\,,$$

replacing ω with s in (1.3), and multiplying by s,

$$\mathrm{D}^{\cos}(s) = \frac{G}{s} - (1+R)s - 32s^3\sum_{n=0}^{\infty}\frac{1}{\gamma_n^3}\frac{T_n}{\left(\gamma_n T_n - 4\delta s^2\right)}\,, \quad (5.14)$$

where for brevity the same symbol, $\mathrm{D}^{\cos}$, is used for the dimensionless characteristic function (5.14).

The complete characteristic function in dimensionless form is the product

$$\Delta^{\cos}(s) = \mathrm{P}^{\cos}(s)\,\mathrm{D}^{\cos}(s)\,, \quad (5.15)$$

with $\mathrm{P}^{\cos}(s)$ the dimensionless form of (5.10),

$$\mathrm{P}^{\cos}(s) = \prod_{m=1}^{\infty}\left(s^2 - m^2\pi^2\frac{\tanh(2m\pi\delta)}{2m\pi\delta}\right). \quad (5.16)$$

5.1 Shallow water limit of $\mathrm{D}^{\cos}$

It is not obvious that the characteristic function (5.14) agrees with the shallow water dispersion relation (1.2). To deduce the shallow water limit, first note that $T_n = \tanh(\gamma_n\delta) \to \gamma_n\delta$ as $\delta \to 0$ for any fixed n, and so formally interchanging the sum and limit

$$\mathrm{D}^{\cos}(s) = \frac{G}{s} - (1+R)s - 32s^3\sum_{n=0}^{\infty}\frac{1}{\gamma_n^3}\frac{\gamma_n}{\left(\gamma_n^2 - 4s^2\right)}\,,$$

again maintaining the same symbol $\mathrm{D}^{\cos}$. To simplify further, two key identities are needed,

$$\frac{\pi^2}{8} = \sum_{n=0}^{\infty}\frac{1}{(2n+1)^2} \quad \text{and} \quad \tan(s) = 8s\sum_{n=0}^{\infty}\frac{1}{(2n+1)^2\pi^2 - 4s^2}\,. \quad (5.17)$$

Now,

$$\frac{4}{\gamma_n^2}\frac{1}{\left(\gamma_n^2-4s^2\right)} = -\frac{1}{s^2\gamma_n^2} + \frac{1}{s^2}\frac{1}{\gamma_n^2-4s^2}\,,$$

and so

$$\mathrm{D}^{\cos}(s) = \frac{G}{s} - Rs - s + s\frac{8}{\pi^2}\sum_{n=0}^{\infty}\frac{1}{(2n+1)^2} - 8s\sum_{n=0}^{\infty}\frac{1}{\left(\gamma_n^2-4s^2\right)}\,.$$

Using the first of (5.17) cancels the third and fourth terms and the second identity in (5.17) shows that the fifth term is $-\tan(s)$. Hence

$$\lim_{\delta\to 0}\mathrm{D}^{\cos}(s) = \frac{G}{s} - Rs - \tan(s) = \mathrm{D}^{\mathrm{SW}}(s)\,.$$

5.2 Roots of the characteristic function $\mathrm{D}^{\cos}$

The roots of the characteristic equation $\mathrm{D}^{\cos}(s) = 0$ give the dimensionless natural frequencies. The simplest approach to finding the *real* roots is to plot $\mathrm{D}^{\cos}(s)$ as a function of s. For each fixed R, G and δ, it is a straightforward numerical calculation to plot $\mathrm{D}^{\cos}(s)$ in (5.14) as a function of s. The only numerical difficulty is avoiding the singularity that occurs for each n at

$$s^2 = \frac{(2n+1)\pi}{4\delta}\tanh((2n+1)\pi\delta)\,. \tag{5.18}$$

The $\mathrm{D}^{\cos}$ versus s curves will be presented in §8.

5.3 Free oscillations of the fluid

Suppose $\widehat{\theta} = 0$ and the vessel is rigidly stationary. Then the only solutions of (5.7)-(5.9) are free oscillations of the fluid: the sloshing modes. There are two classes of free oscillations: anti-symmetric modes with natural frequencies

$$\omega_n^{\mathrm{anti-sym}} = \sqrt{\left(g(2n+1)\frac{\pi}{L}\right)\tanh\left((2n+1)\pi\frac{h_0}{L}\right)}\,, \quad \text{for} \quad n = 0, 1, 2, \ldots\,,$$

and free surface proportional to $\cos\left((2n+1)\frac{\pi}{L}x\right)$, and the symmetric modes with natural frequencies

$$\omega_n^{\mathrm{sym}} = \sqrt{\left(g2n\frac{\pi}{L}\right)\tanh\left(2n\pi\frac{h_0}{L}\right)}\,, \quad \text{for} \quad n = 1, 2, \ldots\,,$$

and free surface proportional to $\cos\left(2n\frac{\pi}{L}x\right)$. Figure 3 shows the free surface profile for the first anti-symmetric and first symmetric modes.

The symmetric modes have the property that $h(L,t)-h(0,t) = 0$ and and the pressure is symmetric about the vessel centerline, giving zero horizontal force on the vessel. On the other hand, the anti-symmetric modes satisfy $h(L,t) - h(0,t) \neq 0$ and they exert a non-trivial force on the vessel. Away from resonance, the anti-symmetric modes are the principal mechanism for coupling between fluid motion and vessel motion. Whereas the symmetric modes, away from resonance, decouple from the vessel motion, but near resonance, the symmetric modes can couple to the vessel motion.

6 Method 3: vertical eigenfunction expansion

Another approach to computing the natural frequencies is to use a *vertical eigenfunction expansion*. This strategy is suggested in §2.1 of LINTON & MCIVER [18], and is used there to solve the forced problem (see §2.2.2 in [18]); that is, (3.9)-(3.10) with $\theta(t)$ considered as given. The boundary value problem (3.9)-(3.10) is solved using the eigenfunction expansion,

$$\widehat{\phi}(x,y) = \sum_{n=0}^{\infty} A_n(x)\psi_n(y)\,, \tag{6.1}$$

where the vertical eigenfunctions satisfy the eigenvalue problem

$$\begin{aligned} -\psi_{yy} &= \lambda\psi\,, \quad 0<y<h_0\,, \\ \psi_y &= 0 \quad \text{at } y=0\,, \\ \psi_y &= \tfrac{\omega^2}{g}\psi \quad \text{at } y=h_0\,. \end{aligned} \tag{6.2}$$

For given ω this boundary value problem has an infinite number of eigenvalues λ_n, and the associated eigenfunctions form a complete set. The first eigenvalue is negative, $\lambda_0 = -k_0^2$ and the rest are positive, $\lambda_n = k_n^2$, $n = 1, 2, \ldots$. The first eigenfunction $\psi_0(y)$ is associated with the *wave mode* and the eigenfunctions $\psi_n(y)$, $n = 1, 2, \ldots$, are associated with the *evanescent modes*. This terminology comes from the wave-maker problem (e.g. §2.2.1 of [18]). The other properties of the eigenfunctions needed here are recorded in Appendix C.

Laplace's equation and the properties of the eigenfunctions give

$$\begin{aligned} A_0(x) &= A_0^{(1)}\cos k_0 x + A_0^{(2)}\sin k_0 x \\ A_n(x) &= A_n^{(1)}\cosh k_n x + A_n^{(2)}\sinh k_n x\,, \quad n = 1, 2, \ldots\,. \end{aligned} \tag{6.3}$$

The coefficients are determined by imposing the boundary conditions at $x = 0$ and $x = L$

$$A_n'(0) = A_n'(L) = \ell\omega\widehat{\theta}\,c_n\,, \quad n = 0, 1, \cdots\,, \tag{6.4}$$

where the expansion $1 = \sum_{n=0}^{\infty} c_n\psi_n(y)$ is used (see (6.21) in §6.4).

The critical equations in this set are the ones for $n = 0$ since they contain information associated with the resonance. The condition (6.4) with $n = 0$ gives

$$A_0^{(2)} = \frac{1}{k_0}\ell\omega\widehat{\theta}c_0\,.$$

The condition at $x = L$ and $n = 0$ requires

$$-2k_0A_0^{(1)}\sin\tfrac{1}{2}k_0L\cos\tfrac{1}{2}k_0L = 2\ell\omega\widehat{\theta}c_0(\sin^2\tfrac{1}{2}k_0L)\,.$$

At this point there is a temptation to impose the assumption

$$\sin\left(\tfrac{1}{2}k_0L\right) \neq 0\,. \tag{6.5}$$

If this assumption is imposed then

$$A_0^{(1)} = -\frac{c_0}{k_0}\tan\left(\tfrac{1}{2}k_0L\right)\ell\omega\widehat{\theta}\,. \tag{6.6}$$

In this case the wave mode ($n = 0$) is intrinsically coupled to the evanescent modes ($n \geq 1$). However, this assumption rules out important resonant solutions. The implications are discussed in §9.

Hence the strategy at this point is to leave both parameters $A_0^{(1)}$ and $\widehat{\theta}$ free with the relation

$$k_0 \sin(k_0 L)\, A_0^{(1)} + \ell\omega\widehat{\theta} c_0 (1 - \cos k_0 L) = 0\,, \tag{6.7}$$

and $A_0(x)$ is left in the general form

$$A_0(x) = A_0^{(1)} \cos k_0 x + \frac{1}{k_0} \ell\omega\widehat{\theta} c_0 \sin k_0 x\,. \tag{6.8}$$

Solving the systems (6.4) for $n \geq 1$ is much simpler as there are no singularities. Solving these equations for the coefficients $A_n^{(1)}$ and $A_n^{(2)}$ results in

$$A_n(x) = \ell\omega\widehat{\theta}\frac{c_n}{k_n} \left(\sinh(k_n x) - \tanh(\tfrac{1}{2} k_n L)\, \cosh(k_n x)\right)\,. \tag{6.9}$$

In this case there is no additional assumption like (6.5) required, since

$$\sinh\left(\tfrac{1}{2} k_n L\right) \neq 0 \quad \text{for all} \quad n \geq 1\,. \tag{6.10}$$

Note that the evanescent modes (6.9) are proportional to $\widehat{\theta}$ and so are intrinsically coupled to the vessel motion.

This completes the construction of the function $\widehat{\phi}(x, y)$ satisfying $\Delta\widehat{\phi} = 0$ and the three boundary conditions (3.10). This solution agrees with the expression for the potential in (2.29) in §2.2.2 of [18].

6.1 Coupling between $\widehat{\theta}$ and $\widehat{\phi}$

Substituting the expansion for $\widehat{\phi}$ into the coupling equation (3.11) gives

$$\begin{aligned} \int_0^L \int_0^{h_0} \rho\widehat{\phi}_x \,\mathrm{d}y\mathrm{d}x \;&=\; \rho c_0 h_0 A_0^{(1)} (\cos(k_0 L) - 1) + \rho h_0 \frac{\ell}{k_0} \omega c_0^2 \sin(k_0 L)\widehat{\theta} \\ &\qquad + 2\rho h_0 \ell\omega\widehat{\theta} \sum_{n=1}^{\infty} \frac{c_n^2}{k_n} \tanh(\tfrac{1}{2} k_n L)\,, \end{aligned}$$

since

$$A_0(L) - A_0(0) = (\cos(k_0 L) - 1) A_0^{(1)} + \frac{\ell}{k_0} \omega c_0 \sin(k_0 L)\, \widehat{\theta}\,,$$

and for $n \geq 1$,

$$A_n(L) - A_n(0) = 2\ell\omega\widehat{\theta}\, \frac{c_n}{k_n} \tanh(\tfrac{1}{2} k_n L)\,.$$

Hence

$$\begin{aligned} \left(\frac{g(m_v + m_f)}{\omega} - m_v \ell\omega\right) \widehat{\theta} \;&=\; \rho c_0 h_0 A_0^{(1)} (\cos(k_0 L) - 1) + \rho h_0 \frac{\ell}{k_0} \omega c_0^2 \sin(k_0 L)\widehat{\theta} \\ &\qquad + 2\rho h_0 \ell\omega\widehat{\theta} \sum_{n=1}^{\infty} \frac{c_n^2}{k_n} \tanh(\tfrac{1}{2} k_n L)\,. \end{aligned} \tag{6.11}$$

The two equations (6.7) and (6.11) are two homogeneous equations for the two unknowns $A_0^{(1)}$ and $\widehat{\theta}$. They can be expressed in matrix form

$$\begin{bmatrix} k_0 \sin(k_0 L) & (1-\cos(k_0 L))\ell\omega c_0 \\ \rho c_0 h_0(\cos(k_0 L)-1) & \Theta \end{bmatrix} \begin{pmatrix} A_0^{(1)} \\ \widehat{\theta} \end{pmatrix} = \begin{pmatrix} 0 \\ 0 \end{pmatrix}, \tag{6.12}$$

where

$$\Theta := \rho \frac{h_0}{k_0} \ell\omega c_0^2 \sin(k_0 L) - \left(\frac{g(m_v+m_f)}{\omega} - m_v \ell\omega \right) + 2\rho h_0 \ell\omega \sum_{n=1}^{\infty} \frac{c_n^2}{k_n} \tanh(\tfrac{1}{2} k_n L)\,. \tag{6.13}$$

The homogeneous equation (6.12) has a solution if and only if the determinant of the coefficient matrix vanishes. This condition provides the characteristic equation $\Delta^{\rm vert}(\omega) = 0$ where

$$\Delta^{\rm vert}(\omega) = \det \begin{bmatrix} k_0 \sin(k_0 L) & (1-\cos(k_0 L))\ell\omega c_0 \\ \rho c_0 h_0(\cos(k_0 L)-1) & \Theta \end{bmatrix},$$

or

$$\Delta^{\rm vert} = k_0 \sin(k_0 L)\Theta + \rho h_0 \ell\omega c_0^2 (1-\cos(k_0 L))^2\,.$$

After some algebra, this condition can be written in the form

$$\Delta^{\rm vert}(\omega) = 2k_0 \sin\left(\tfrac{1}{2} k_0 L\right) \cos\left(\tfrac{1}{2} k_0 L\right) \mathrm{D}^{\rm vert}(\omega)\,,$$

with

$$\begin{aligned} \mathrm{D}^{\rm vert}(\omega) \;\; = \;\; & -\left(\frac{g(m_v+m_f)}{\omega} - m_v \ell\omega \right) + 2\rho \frac{h_0}{k_0} \ell\omega c_0^2 \tan(\tfrac{1}{2} k_0 L) \\ & + 2\rho h_0 \ell\omega \sum_{n=1}^{\infty} \frac{c_n^2}{k_n} \tanh(\tfrac{1}{2} k_n L)\,. \end{aligned} \tag{6.14}$$

The factor $k_0 \cos\left(\frac{1}{2} k_0 L\right)$ is never zero. This property follows by noting that $k_0 = 0$ is not a solution of the characteristic equation (C-3) for $\omega \neq 0$ and the product $\cos\left(\frac{1}{2} k_0 L\right) \mathrm{D}^{\rm vert}$ is strictly positive when $\frac{1}{2} k_0 L$ is an odd multiple of $\frac{1}{2}\pi$. Hence the appropriate characteristic function is

$$\Delta^{\rm vert}(\omega) = \mathrm{P}^{\rm vert}(\omega)\, \mathrm{D}^{\rm vert}(\omega)\,, \quad \text{with} \quad \mathrm{P}^{\rm vert}(\omega) := \sin\left(\tfrac{1}{2} k_0 L\right). \tag{6.15}$$

The characteristic function is a bit easier to interpret if it is made dimensionless. Introduce the scaling (1.4). Then

$$\left(\frac{g(m_v+m_f)}{\omega} - m_v \ell\omega \right) = 2m_f \frac{\ell}{L} \sqrt{g h_0} \left(\frac{G}{s} - Rs \right).$$

Substitute into (6.14) and divide by $-2m_f \ell L^{-1} \sqrt{g h_0}$,

$$\mathrm{D}^{\rm vert}(s) = \left(\frac{G}{s} - Rs \right) - s \frac{2c_0^2}{k_0 L} \tan(\tfrac{1}{2} k_0 L) - s \sum_{n=1}^{\infty} \frac{2c_n^2}{k_n L} \tanh(\tfrac{1}{2} k_n L)\,, \tag{6.16}$$

where for brevity the same symbol $\mathrm{D}^{\rm vert}$ is used.

The factor $\mathrm{D}^{\mathrm{vert}}$ in (6.16) agrees with the result derived by Yu [25]. The derivation in [25] implicitly uses a vertical eigenfunction expansion. By translating the notation in [25] to the notation here it can be shown that the expression for the characteristic equation in [25] agrees with $\mathrm{D}^{\mathrm{vert}}$. However, the characteristic equation in [25] is missing the factor $\sin(\frac{1}{2}k_0(s)L)$ in (6.15).

The complete dimensionless characteristic function is

$$\Delta^{\mathrm{vert}}(s) = \mathrm{P}^{\mathrm{vert}}(s)\,\mathrm{D}^{\mathrm{vert}}(s)\,, \quad \text{with} \quad \mathrm{P}^{\mathrm{vert}}(s) := \sin\left(\tfrac{1}{2}k_0(s)L\right), \tag{6.17}$$

with $\mathrm{D}^{\mathrm{vert}}(s)$ defined in (6.16). It is remarkable that the two representations of the characteristic equation (6.16) and (5.14) have the same roots. A proof of this equivalence is given in §7, and this equivalence is seen in the numerical results as well (see below in §8).

6.2 Shallow water limit of $\mathrm{D}^{\mathrm{vert}}$

In the shallow water limit, the function $\mathrm{D}^{\mathrm{vert}}(s)$ in (6.16) should reduce to $\mathrm{D}^{\mathrm{SW}}(s)$ in (1.2). To see this non-dimensionalize (C-3),

$$\delta k_0 L \tanh(\delta k_0 L) - 4\delta^2 s^2 = 0\,.$$

Hence, for fixed δ, this equation is solved for k_0L as a function of s,

$$\frac{k_0 L}{4\delta}\tanh(\delta k_0 L) = s^2\,. \tag{6.18}$$

In the limit $\delta \to 0$, with s and L fixed, the above function gives

$$s = \tfrac{1}{2}k_0 L\,.$$

Scale the coefficient c_0 in (6.21)

$$c_0 = \frac{1}{N_0}\frac{\sinh(k_0 h_0)}{k_0 h_0} = \frac{1}{N_0}\frac{\sinh(k_0 L\delta)}{k_0 L\delta} \to \frac{1}{N_0} \quad \text{as } \delta \to 0\,.$$

By a similar argument it follows that $N_0 \to 1$ and so $c_0 \to 1$ in the limit $\delta \to 0$. Hence

$$\lim_{\delta\to 0}\mathrm{D}^{\mathrm{vert}}(s) = \left(\frac{G}{s} - Rs\right) - \tan(s) - s\lim_{\delta\to 0}\sum_{n=1}^{\infty}\frac{c_n^2}{\frac{1}{2}k_n L}\tanh(\tfrac{1}{2}k_n L)\,.$$

If the sum on the right hand side vanishes,

$$\lim_{\delta\to 0}\mathrm{D}^{\mathrm{vert}}(s) = \mathrm{D}^{\mathrm{SW}}(s)\,.$$

The sum involves evanescent modes and the proof that the sum vanishes in the limit $\delta \to 0$ requires careful analysis of the relation between k_n for $n \geq 1$ and s (C-5).

6.3 Roots of the characteristic equation $\mathrm{D}^{\mathrm{vert}}$

The characteristic equation for the coupled modes, $\mathrm{D}^{\mathrm{vert}}(s) = 0$, depends on the parameters G, R, and δ. When these three parameters are fixed, the characteristic equation is a function of s only. The dimensionless wavenumbers k_0L and k_nL are determined as functions of s and δ through the equations (C-3) and (C-5) defined in Appendix C. The dimensionless wavenumber k_0L is determined by solving (6.18). To determine k_n for $n \geq 1$, scale (C-5) to

$$0 = \delta kL \tan(\delta kL) + 4\delta^2 s^2 \,. \tag{6.19}$$

This equation is solved for each k_nL as a function of s, with δ fixed,

$$\frac{k_nL}{4\delta}\tan(\delta k_nL) = -s^2 \,.$$

The Fourier coefficients c_n, $n \geq 0$, also depend on k_n and so in turn depend on s. Hence, with fixed G, R and δ, the characteristic equation (6.17) depends only on s, albeit in a very complicated way. Therefore, evaluating $\mathrm{D}^{\mathrm{vert}}(s)$ as a function of s is a much more complicated numerical undertaking, especially when compared with $\mathrm{D}^{\cos}(s)$.

6.4 Expansion of the function $f(y) = 1$

In the implementation of the boundary conditions at $x = 0$ and $x = L$, the expansion of the function $f(y) = 1$ was used. Theoretically this expansion is elementary, but there are practical difficulties.

The function $f(y) = 1$ is square integrable and so the infinite expansion in terms of the vertical eigenfunctions exists and converges. Using the theory in Appendix C,

$$1 = \sum_{n=0}^{\infty} c_n \psi_n(y) \,, \tag{6.20}$$

with coefficients

$$c_0 = \frac{1}{N_0}\frac{\sinh k_0h_0}{k_0h_0} \quad \text{and} \quad c_n = \frac{1}{N_n}\frac{\sin k_nh_0}{k_nh_0} \,, \tag{6.21}$$

with N_n, $n = 0, 1, \ldots$, defined in (C-7). On the other hand the theory states that the sum on the right-hand side of (6.20) equals the function on the left *almost everywhere on the interval* $[0, h_0]$. Define the sum on the right hand side of (6.20) by

$$\mathsf{S}(y) = \sum_{n=0}^{\infty} c_n \psi_n(y) \,.$$

Then since $\psi_n(y)$ satisfies $\psi_n'(y) = \frac{\omega^2}{g}\psi_n(y)$ when $y = h_0$ (cf. (6.2)), it follows that $S(h_0) = 0$. Hence the series on the right-hand side of (6.20) does not represent the function $f(y) = 1$. It represents

$$f(y) = \begin{cases} 0 & \text{for } y = h_0 \\ 1 & \text{for } 0 \leq y < h_0 \,. \end{cases}$$

The practical implication of this is that the series converges very slowly, and has Gibbs-type oscillations near $y = h_0$. Examples are shown in Figures 4 and 5.

Fixing $\omega = 2.1$ and the value of δ, the eigenvalues of (6.2) are obtained numerically as outlined in §8. In Figure 4 the depth ratios is set at $\delta = 0.1$. There are 3 lines on each figure, these correspond to $M = 10$, 50 and 100, showing clear increased accuracy at $y = h_0$ ($y = 1$ in the figures since the y axis is scaled to the interval $[0, 1]$). In Figure 5 the depth ratio is set at $\delta = 1.0$. The results improve with decreasing δ with the shallow water result clearly converging much faster than the deep water result. However, in all cases there is non-trivial error at $y = h_0$ even with $M = 100$. This poor convergence of

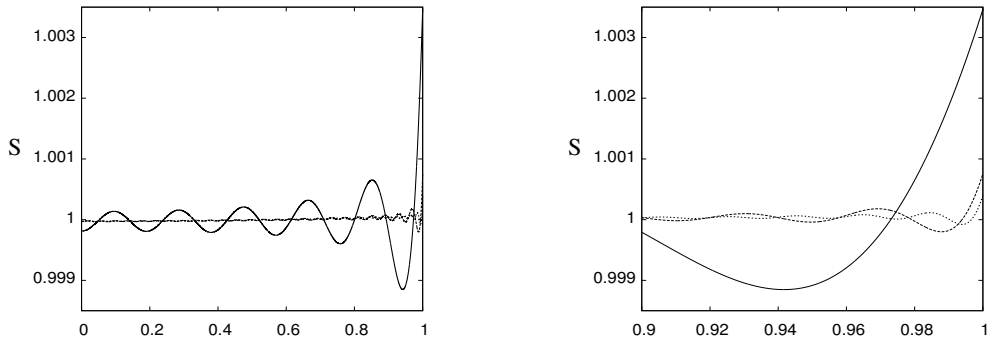

(a) (b)

Figure 4: Plot of the sum $S(y/h_0)$ representing the function $f(y) = 1$ when $\delta = 0.1$ with (a) plot over the entire interval and (b) a close up near $y = h_0$.

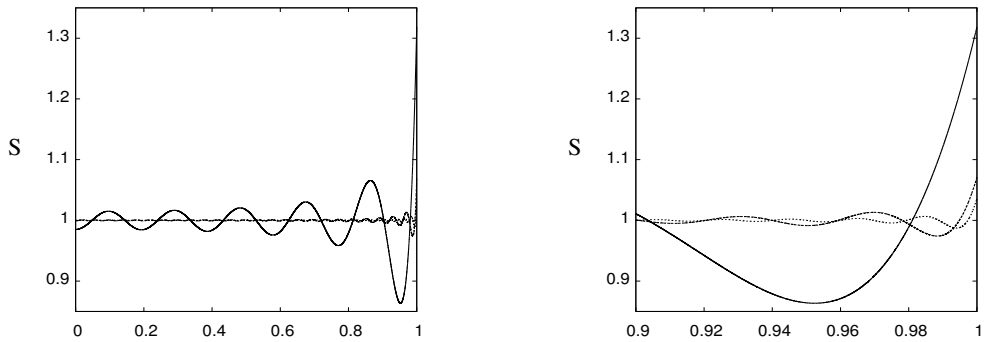

(a) (b)

Figure 5: Plot of the sum $S(y/h_0)$ representing the function $f(y) = 1$ when $\delta = 1.0$ with (a) plot over the entire interval and (b) a close up near $y = h_0$.

the series representation of $f(y) = 1$ is one of the weaknesses of the vertical eigenfunction expansion, since the coefficients c_n appear in a central way.

7 Equivalence of the cosine and vertical eigenfunction representations

The strategy for showing equivalence between the cosine expansion (5.6) and the vertical eigenfunction expansion (6.1) is to expand the $y-$dependence of (5.6) in terms of the

vertical eigenfunctions and expand the $x-$dependent functions $A_n(x)$ in (6.1) in terms of a cosine series, and then compare the two. This strategy for the proof was suggested to the authors by McIver [19].

For simplicity restrict to non-resonant modes. The extension to resonant modes follows the same lines.

The cosine expansion with $b_n = 0$ can be written in the form

$$\widehat{\phi}(x,y) = \ell\omega\widehat{\theta}\sum_{m=0}^{\infty} p_m\, f_m(y)\, \cos(\alpha_m x)\,, \tag{7.1}$$

with

$$f_m(y) = 1 + \left(\frac{K}{K_m - K}\right)\frac{\cosh(\alpha_m y)}{\cosh(\alpha_m h_0)}\,, \tag{7.2}$$

where

$$K := \frac{\omega^2}{g} \quad \text{and} \quad K_m := \alpha_m \tanh(\alpha_m h_0)\,.$$

Expand $f_m(y)$ in terms of the vertical eigenfunctions

$$f_m(y) = 1 + \left(\frac{K}{K_m - K}\right)\frac{\cosh(\alpha_m y)}{\cosh(\alpha_m h_0)} = \sum_{n=0}^{\infty} F_n^{(m)}\,\psi_n(y)\,. \tag{7.3}$$

The coefficients $F_n^{(m)}$ are determined using the formulae (C-10)

$$F_0^{(m)} = c_0\,\frac{\alpha_m^2}{\alpha_m^2 - k_0^2} \quad \text{and} \quad F_n^{(m)} = c_n\frac{\alpha_m^2}{k_n^2 + \alpha_m^2}\,. \tag{7.4}$$

Similarly expand the functions $A_0(x)$ in (6.8) (using (6.6)) and $A_n(x)$ in (6.9). For $A_0(x)$,

$$A_0(x) := \ell\omega\widehat{\theta}\frac{c_0}{k_0}\big(\sin(k_0 x) - \tan\left(\tfrac{1}{2}k_0 L\right)\cos(k_0 x)\big) = \sum_{m=0}^{\infty} u_m\,\cos(\alpha_m x)\,, \tag{7.5}$$

with

$$u_m = \ell\omega\widehat{\theta}c_0 p_m\frac{\alpha_m^2}{\alpha_m^2 - k_0^2}\,, \tag{7.6}$$

where $p_m = -4/L\alpha_n^2$ are the coefficients of the cosine expansion of $x - L/2$ in (5.5). Similarly, using (6.9),

$$A_n(x) = \ell\omega\widehat{\theta}\frac{c_n}{k_n}\big(\sinh(k_n x) - \tanh\left(\tfrac{1}{2}k_n L\right)\cosh(k_n x)\big) = \sum_{m=0}^{\infty} U_m^{(n)}\,\cos(\alpha_m x)\,, \tag{7.7}$$

with

$$U_m^{(n)} = \ell\omega\widehat{\theta}c_n p_m\frac{\alpha_m^2}{k_n^2 + \alpha_m^2}\,. \tag{7.8}$$

To show equivalence between the two representations start with the cosine expansion. Substitute the vertical eigenfunction expansion for $f_m(z)$, reverse the order of summation,

and then substitute the cosine expansion of the sequence of functions $A_n(x)$. The result is the vertical eigenfunction representation. Carrying out the above steps:

$$\begin{aligned}
\widehat{\phi}(x,y) &= \ell\omega\widehat{\theta}\big(x-\tfrac{1}{2}L\big)+\sum_{n=0}^{\infty}a_n\frac{\cosh(\alpha_n y)}{\cosh(\alpha_n h_0)}\,\cos(\alpha_n x)\\
&= \ell\omega\widehat{\theta}\sum_{n=0}^{\infty}p_n\cos(\alpha_n x)+\ell\omega\widehat{\theta}\sum_{n=0}^{\infty}p_n\left(\frac{K}{K_n-K}\right)\frac{\cosh(\alpha_n y)}{\cosh(\alpha_n h_0)}\,\cos(\alpha_n x)\\
&= \ell\omega\widehat{\theta}\sum_{n=0}^{\infty}p_n f_n(y)\cos(\alpha_n x)\\
&= \ell\omega\widehat{\theta}\sum_{n=0}^{\infty}\sum_{m=0}^{\infty}p_n F_m^{(n)}\psi_m(y)\,\cos(\alpha_n x)\\
&= \ell\omega\widehat{\theta}\sum_{m=0}^{\infty}\sum_{n=0}^{\infty}p_m F_n^{(m)}\psi_n(y)\,\cos(\alpha_m x)\\
&= \ell\omega\widehat{\theta}\sum_{m=0}^{\infty}p_m F_0^{(m)}\psi_0(y)\,\cos(\alpha_m x)+\ell\omega\widehat{\theta}\sum_{n=1}^{\infty}\sum_{m=0}^{\infty}p_m F_n^{(m)}\psi_n(y)\,\cos(\alpha_m x)\\
&= \ell\omega\widehat{\theta}c_0\psi_0(y)\sum_{m=0}^{\infty}p_m\frac{\alpha_m^2}{\alpha_m^2-k_0^2}\cos(\alpha_m x)+\ell\omega\widehat{\theta}\sum_{n=1}^{\infty}\sum_{m=0}^{\infty}p_m c_n\frac{\alpha_m^2}{k_n^2+\alpha_m^2}\psi_n(y)\,\cos(\alpha_m x)\\
&= \psi_0(y)\sum_{m=0}^{\infty}u_m\cos(\alpha_m x)+\sum_{n=1}^{\infty}\sum_{m=0}^{\infty}U_m^{(n)}\psi_n(y)\,\cos(\alpha_m x)\\
&= \left[\sum_{m=0}^{\infty}u_m\cos(\alpha_m x)\right]\psi_0(y)+\sum_{n=1}^{\infty}\left[\sum_{m=0}^{\infty}U_m^{(n)}\cos(\alpha_m x)\right]\psi_n(y)\\
&= A_0(x)\psi_0(y)+\sum_{n=1}^{\infty}A_n(x)\psi_n(y)\,,
\end{aligned}$$

which is the representation of $\widehat{\phi}$ in terms of vertical eigenfunction expansion. This completes the transformation from the cosine expansion to the vertical eigenfunction expansion.

A similar argument can show that characteristic functions $\mathrm{D}^{\cos}(s)$ and $-\mathrm{D}^{\mathrm{vert}}(s)$ are equivalent (the form of $\mathrm{D}^{\mathrm{vert}}(s)$ in (6.14) must be multiplied by -1 in order to show equivalence). The main aspect of the proof is to show that the horizontal momentum of the fluid $\mathsf{M}^{\mathrm{horz}}$ is equivalent for each expansion. The detailed proof of this is given in the technical report [6], and the main result quoted here is

$$\mathsf{M}^{\mathrm{horz}}=m_f\left[1-\frac{1}{h_0L}\sum_{n=0}^{\infty}2\frac{p_n}{\alpha_n^2}\left(\frac{KK_n}{K_n-K}\right)\right]=m_f\left[2\frac{c_0^2}{k_0L}\tan\left(\tfrac{1}{2}k_0L\right)+\sum_{n=1}^{\infty}2\frac{c_n^2}{k_nL}\tanh\left(\tfrac{1}{2}k_nL\right)\right].$$

The equivalence of the two characteristic functions (5.13) and (6.14) is now clear by

writing

$$\begin{aligned}
\mathrm{D}^{\cos} &= \Big((m_v+m_f)\frac{g}{\omega}-m_v\ell\omega\Big)-\ell\omega m_f-\frac{8\ell m_f\omega^3}{L^2h_0g}\sum_{n=0}^{\infty}\frac{1}{\alpha_n^2}\frac{\tanh\alpha_nh_0}{\alpha_n\tanh\alpha_nh_0-\omega^2/g}\,,\\
&= \Big((m_v+m_f)\frac{g}{\omega}-m_v\ell\omega\Big)-\ell\omega m_f\left[1-\frac{1}{h_0L}\sum_{n=0}^{\infty}2\frac{p_n}{\alpha_n^2}\left(\frac{KK_n}{K_n-K}\right)\right],\\
&= \Big((m_v+m_f)\frac{g}{\omega}-m_v\ell\omega\Big)-\ell\omega m_f\left[2\frac{c_0^2}{k_0L}\tan\left(\tfrac{1}{2}k_0L\right)+\sum_{n=1}^{\infty}2\frac{c_n^2}{k_nL}\tanh\left(\tfrac{1}{2}k_nL\right)\right],\\
&= \Big((m_v+m_f)\frac{g}{\omega}-m_v\ell\omega\Big)-\frac{2\ell\omega m_fc_0^2}{k_0L}\tan\left(\tfrac{1}{2}k_0L\right)-2\ell\omega m_f\sum_{n=1}^{\infty}\frac{c_n^2}{k_nL}\tanh\left(\tfrac{1}{2}k_nL\right)\Bigg],\\
&= -\mathrm{D}^{\mathrm{vert}},
\end{aligned}$$

with $m_f=\rho h_0L$.

8 Numerical evaluation of the characteristic equation

The simplest way to get approximate values for the real roots is to plot them as functions of s. The approximate values can then be refined if necessary using Newton's method.

Plotting $\mathrm{D}^{\cos}$ as a function of s, for fixed G, R and δ, is straightforward and requires no special numerical technique. The terms in the sum are evaluated and summed, with special care needed only near the singularities (5.18). The numerical results retain 50 terms in the summation to give results with agree with the vertical eigenfunction expansion to a high degree of accuracy.

Plotting $\mathrm{D}^{\mathrm{vert}}$ as a function of s is a much more difficult undertaking. The principal difficulty is computing the wavenumbers $k_0(s)$ and $k_n(s)$, for $n=1,2,\ldots$. The obvious numerical strategy is to solve the transcendental equation $\mathsf{C}(\lambda)=0$ in (C-1). Firstly, this approach requires an accurate initial guess for each wavenumber for the iterative method to converge, and secondly one must be certain that no wavenumbers are missed.

Other approximate and numerical methods for computing these wavenumbers have been developed. For example, Chamberlain & Porter [8] compute approximations for the wavenumbers by constructing an integral equation for the eigenfunctions and then solving the integral equation both analytically and numerically. We use a similar strategy, except we approximate the differential equation (6.2) directly. Since the domain is finite, Chebyshev polynomial expansions can be used to approximate the $\psi_n(y)$ eigenfunctions for each n with high accuracy.

8.1 Spectral solution of the vertical eigenfunctions

Fix G, R and δ. Then at each value of s, the values of $k_0(s)$ and $k_m(s)$ need to be determined for $m=1,..,M$, where M is a large enough integer such that $\mathrm{D}^{\mathrm{vert}}$ is independent of M. The strategy here is to expand the eigenfunctions $\psi_n(y)$ in a series of Chebyshev polynomials (cf. Boyd [7]), converting (6.2) to a matrix eigenvalue problem. Then a global eigenvalue solver gives all the eigenvalues up to the degree of the Chebyshev polynomial. In this approach the $y-$domain is transformed from $y\in[0,h_0]$ to $\bar{y}\in[-1,1]$

and we assume that

$$\psi(\bar{y}) = \sum_{i=0}^{N_C} a_i T_i(\bar{y}),$$

where $T_i(\bar{y})$ are Chebyshev polynomials, and a_i are undetermined parameters. Evaluating this expression at the $N_C - 1$ collocation points

$$\bar{y}_i = \cos\left(\frac{i\pi}{N_C}\right), \quad i = 1, ..., N_C - 1,$$

and at the two boundaries $\bar{y} = -1$ and $\bar{y} = 1$, gives $N_C + 1$ algebraic equations for the eigenvalues λ, reducing (6.2) to the matrix eigenvalue problem

$$\mathbf{A}\Psi = \lambda\Psi\,, \quad \Psi \in \mathbb{R}^{N_c+1}\,.$$

The eigenvalues of $\mathbf{A}$ are then found via a standard QR-algorithm. We used the standard QR eigenvalue solver from LAPACK. The main benefit of this approach is that all the required eigenvalues, and hence the values of $k_0, k_1, \ldots$ are calculated in one go, without missing any. By choosing N_c large enough, the first M modes can be calculated to the desired accuracy.

The results in this paper use $M = 10$ evanescent modes, and so using $N_C = 50$ in the spectral collocation approach above is sufficient to calculate the values of $k_0, k_1, \ldots$ to 12 significant figures. These computed values were checked against values calculated via an iterative solution of (C-1).

8.2 Plotting $\mathrm{D}^{\mathrm{vert}}(s)$ as a function of s

To determine the sequence of dimensionless natural frequencies s_j, for $j = 1, 2, \ldots$, for which $\mathrm{D}^{\cos}(s_j) = 0$ or $\mathrm{D}^{\mathrm{vert}}(s_j) = 0$, we plot $\mathrm{D}^{\mathrm{vert}}$ and $\mathrm{D}^{\cos}$ as a function of s and then calculate when this function crosses the $s-$axis. As a test of the numerics we plotted both and to graphical accuracy they were identical which provides a check on the numerics. Therefore we just plot $\mathrm{D}^{\mathrm{vert}}(s)$ henceforth.

For $n = 1$ $\mathrm{D}^{\mathrm{vert}}$ is plotted in Figure 6. Once a root of $\mathrm{D}^{\mathrm{vert}}(s) = 0$ is found, the values of $k_0, k_1, \ldots$ at that point can then be used to plot other features such as the surface elevation $h(x, t)$.

In the shallow water limit, Figure 6(a), the roots of the characteristic function are evenly spaced, as there is negligible contribution from the evanescent modes in this limit. While for a finite depth fluid in Figure 6(b), the spacing between the roots of the characteristic function reduces as s increases due to the presence of evanescent modes.

8.3 Effect of coupling on free surface mode shapes

The free surface mode shapes for the first anti-symmetric and first symmetric free oscillation modes are just simple cosine functions (cf. Figure 3).

When the fluid motion is coupled to the vessel motion the free surface can be much more complicated since the full Fourier series or full eigenfunction expansion comes into play. In this section some mode shapes for the free surface when it is fully coupled are

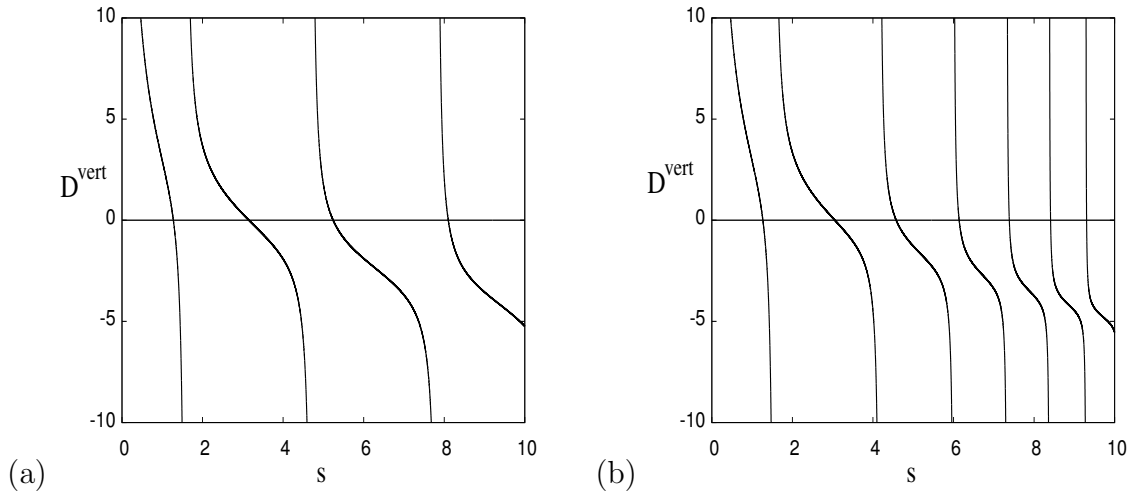

Figure 6: Dispersion relations $\mathrm{D}^{\mathrm{vert}}(s)$ and $\mathrm{D}^{\cos}(s)$ (which exactly overlap) with $G = 5$ and $R = \frac{1}{2}$ for (a) $\delta = 0.01$ and (b) $\delta = 0.1$.

presented. The free surface mode shapes are defined in (3.8). Using the representation in terms of the vertical eigenfunctions the non-dimensional free surface mode shape is

$$h(x/L)/h_0 = 1 + \frac{(1+R)s^2}{G\delta} \sum_{n=0}^{\infty} \widehat{A}_n(x/L)\psi_n(h_0)\,.$$

In the fully coupled non-resonant case,

$$\begin{aligned} \widehat{A}_0(x/L) &= \widehat{\theta}_{\frac{c_0}{k_0 L}} \left(\sin(Lk_0 x/L) - \tan(\tfrac{1}{2}k_0 L)\cos(Lk_0 x/L)\right) \\ \widehat{A}_n(x/L) &= \widehat{\theta}_{\frac{c_n}{k_n L}} \left(\sinh(Lk_n x/L) - \tanh(\tfrac{1}{2}k_n L)\cosh(Lk_n x/L)\right)\,, \quad n \geq 1\,. \end{aligned}$$

Examples are shown in the following figures. Although a very large number of terms is included the effect of the higher modes on the free surface shape is minor. The free surface shape for the coupled modes is still very close to a cosine function.

9 Internal 1:1 resonance

There is an internal $1:1$ resonance in the finite depth model, and it can be deduced from either the vertical eigenfunction expansion or the cosine expansion. The derivation in the former case follows closely the analysis in the shallow water case, and so it is considered first. The $1:1$ resonance occurs when the two factors in the product representation (6.17) vanish simultaneously,

$$\mathrm{P}^{\mathrm{vert}}(s) = 0 \quad \text{and} \quad \mathrm{D}^{\mathrm{vert}}(s) = 0\,. \tag{9.1}$$

Vanishing of the first factor gives

$$k_0 L = 2m\pi \quad \text{for any integer } m\,. \tag{9.2}$$

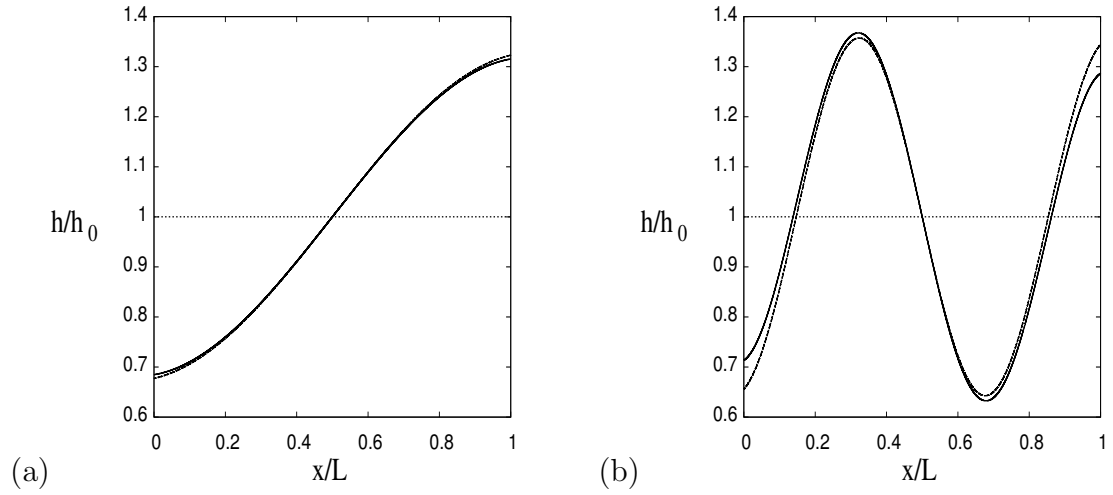

Figure 7: A plot of the free surface when $G = 5\,,\ R = 0.5\,,\ \delta = 0.5\,,$ and $\widehat{\theta} = \pi/20$ for (a) the 1st root of the characteristic function $\mathrm{D}^{\mathrm{vert}}(s)$ and (b) the second root of $\mathrm{D}^{\mathrm{vert}}(s)$. The solid line is the profile including evanescent modes and he dashed line is just the wave mode and the dotted line is $y = h_0\,.$

Using (6.18), the value of s is

$$s_m = m\pi\sqrt{\frac{\tanh\,(2m\pi\delta)}{2m\pi\delta}}\,. \tag{9.3}$$

This sequence of values of s is associated with symmetric sloshing modes (cf. §5.3).

With the condition (9.2) the equation (6.7) is exactly satisfied. The second equation (6.11) is equivalent to the the vanishing of the second factor in (9.1). Including the factor $\widehat{\theta}$, the required condition is

$$\left[-\left(\frac{g(m_v + m_f)}{\omega} - m_v\ell\omega\right) + 2\rho h_0\ell\omega\sum_{n=1}^{\infty}\frac{c_n^2}{k_n}\tanh(\tfrac{1}{2}k_nL)\right]\widehat{\theta} = 0\,. \tag{9.4}$$

There are two solutions: $\widehat{\theta} = 0$ and the vessel is stationary, and $\widehat{\theta} \neq 0$, and then the term in brackets should vanish. The condition $\widehat{\theta} = 0$ makes the vessel stationary, and the fluid motion reduces to just free oscillation, with no horizontal force acting on the vessel. The solution with $\widehat{\theta} \neq 0$ is much more interesting. Making the term in brackets in (9.4) dimensionless, and setting it to zero, gives

$$\frac{G}{s} = Rs + s\sum_{n=1}^{\infty}\frac{c_n^2}{\frac{1}{2}k_nL}\tanh(\tfrac{1}{2}k_nL)\,. \tag{9.5}$$

In this equation s is fixed by the choice of m in (9.3) and this choice in turn determines the values of k_n for $n \geq 1$ via

$$k_n^2L^2\frac{\tan(\delta k_nL)}{\delta k_nL} = -4m^2\pi^2\frac{\tanh\,(2m\pi\delta)}{2m\pi\delta}\,.$$

Hence for fixed m in (9.2) and fixed δ the condition (9.5) gives a line in the (R, G) plane along which there is a resonance. Calculations for a range of δ values are shown in Figure

8. In all cases the resonance curve is a straight line. In the limit of shallow water it has a steep slope and passes through the origin. As δ increases the slope decreases and the $G-$intercept increases, to the point where the line is almost vertical in the limit of deep water. As δ ranges from shallow water to deep water, a dense region of the (R, G) parameter space is covered.

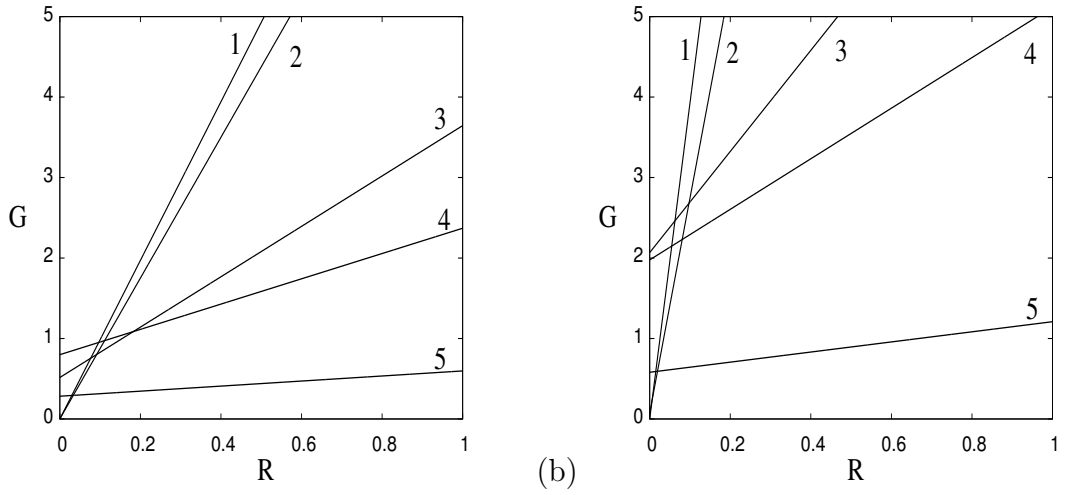

Figure 8: Plot of the (a) the first $(m = 1)$ and (b) the second $(m = 2)$ resonance curve in the $(G, R)-$plane, for $\delta = 0.01,\ 0.1,\ 0.5,\ 1.0$ and 5.0 numbered $1 - 5$ respectively.

To confirm the necessary condition for a $1:1$ resonance; that is, it corresponds to a double natural frequency of the characteristic equation, check that the derivative vanishes,

$$\Delta^{\rm vert}(s) = \frac{d}{ds}\Delta^{\rm vert}(s) = 0\,. \tag{9.6}$$

But if s satisfies (9.3), then

$$\frac{d}{ds}\Delta^{\rm vert}(s)\bigg|^{s=s_m} = \tfrac{1}{2}\,L(-1)^m k_0'(s_m)\,{\rm D}^{\rm vert}(s_m)\,,$$

and since $k_0'(s) \neq 0$ it follows that a $1:1$ resonance occurs when $\sin(\frac{1}{2}k_0 L) = 0$ and ${\rm D}^{\rm vert}(s_m) = 0$, but ${\rm D}^{\rm vert}(s_m) = 0$ is precisely the condition (9.5) with $s = s_m$.

9.1 The eigenfunctions at resonance in finite depth

This $1:1$ resonance is semisimple. There are two linearly independent eigenfunctions parameterized by $A_0^{(1)}$ and $\widehat{\theta}$. In the linear problem any combination of the two eigenfunctions is admissible. On the other hand, a weakly nonlinear analysis near this resonance will single out particular families of solutions (see discussion in §10). The eigenfunctions for $\theta(t)$ and $\phi(x, y, t)$ for each m are

$$\begin{aligned} \theta_m(t) &= \widehat{\theta}\sin(\omega_m t), \\ \phi_m(x, y, t) &= \widehat{\phi}(x, y)\cos(\omega_m t)\,, \end{aligned} \tag{9.7}$$

with $\omega_m = \frac{2}{L}\sqrt{gh_0}s_m$, and $\widehat{\phi}(x,y) = \sum_{n=0}^{\infty} A_n(x)\psi_n(y)$. Now separate $\widehat{\phi}$ into two parts, one proportional to $A_0^{(1)}$ and the other proportional to $\widehat{\theta}$,

$$\widehat{\phi}(x,y) = A_0^{(1)}\widehat{\phi}_1^{\text{vert}}(x,y) + \ell\omega\widehat{\theta}\,\widehat{\phi}_2^{\text{vert}}(x,y)\,,$$

with

$$\widehat{\phi}_1^{\text{vert}}(x,y) = \cos(k_0 x)\psi_0(y), \tag{9.8}$$

and

$$\widehat{\phi}_2^{\text{vert}}(x,y) = \frac{c_0}{k_0}\sin(k_0 x)\,\psi_0(y) + \sum_{n=1}^{\infty}\frac{c_n}{k_n}\left(\sinh(k_n x) - \tanh(\tfrac{1}{2}k_n L)\,\cosh(k_n x)\right)\psi_n(y)\,. \tag{9.9}$$

At the $1:1$ resonance, the two parameters $A_0^{(1)}$ and $\widehat{\theta}$ are arbitrary. The solutions with $\widehat{\theta} = 0$ are the free oscillations with the vessel stationary and no contribution from the evanescent modes. The solutions with $A_0^{(1)} = 0$ are quite different in that the fluid motion and vessel motion are coupled. There is then a continuum of mixed modes obtained by taking arbitrary values of $A_0^{(1)}$ and $\widehat{\theta}$ (determined by the choice of initial data).

9.2 1:1 resonance in the cosine formulation

The $1:1$ resonance in the cosine formulation is obtained by setting the two factors in (5.15) to zero simultaneously. Setting the first factor to zero amounts to choosing a symmetric fluid mode; that is, for some $m \in \mathbb{N}$, $b_m \neq 0$ and $b_n = 0$ for all $n \neq m$, and

$$\omega_m^2 = g\beta_m \tanh(\beta_m h_0)\,.$$

In dimensionless form,

$$s_m = m\pi\sqrt{\frac{\tanh(2m\pi\delta)}{2m\pi\delta}}\,, \tag{9.10}$$

agreeing with the result found using the vertical eigenfunction expansion (9.3). The expression for a_n in (5.8) then becomes

$$a_n = -4\frac{\ell}{L}\omega\widehat{\theta}\frac{s_m^2}{\alpha_n^2}\frac{1}{\sigma_{m,n}}\,, \tag{9.11}$$

where

$$\sigma_{m,n} = \left[\frac{(2n+1)}{2}\pi\right]^2\frac{\tanh(\alpha_n h_0)}{\alpha_n h_0} - s_m^2\,.$$

Substitution into (5.9) and scaling gives

$$\left[\frac{G}{s_m^2} - R - 1 - \frac{8}{\delta}s_m^2\sum_{n=0}^{\infty}\frac{\tanh(\alpha_n h_0)}{(\alpha_n L)^3\sigma_{m,n}}\right]\widehat{\theta} = 0\,. \tag{9.12}$$

This equation is the analogue in the cosine formulation of (9.4). If $\widehat{\theta} = 0$ then the vessel is stationary and a symmetric free mode exists. If $\widehat{\theta} \neq 0$ then there is a line in the

$(R,G)-$plane where a resonance between the vessel motion and the symmetric mode exists,

$$G = s_m^2 R + s_m^2 + \frac{8}{\delta} s_m^4 \sum_{n=0}^{\infty} \frac{\tanh((2n+1)\pi\delta)}{(2n+1)^3 \pi^3 \, \sigma_{m,n}} \,. \tag{9.13}$$

It follows from the equivalence proof that this expression is exactly equal to (9.5). Details of the equivalence argument are given in the technical report [6].

In the limit $\delta \to 0$ the second and third terms on the right-hand side vanish (using the identities (5.17)) and $s_m \to m\pi$, reducing (9.13) to the shallow water condition (1.6).

To show that the resonance line (9.13) reduces to the resonance line in the Ikeda-Nakagawa formulation (4.10) truncate the sum to the first term in (9.13) and take $s_m = s_0$, where s_0 is defined in (4.9),

$$\frac{G}{s_0} - s_0 R = s_0 + \frac{8}{\delta} s_0^3 \frac{\tanh(\pi\delta)}{\pi^3 \, \sigma_{0,0}} = s_0 + 8 s_0^3 \frac{\mathcal{T}_0}{\pi^2 \, (\frac{1}{4}\pi^2 \mathcal{T}_0 - s_0^2)} \,,$$

which agrees with (4.10), noting that $\alpha_0 L = \pi$.

The representation for the two eigenfunctions in this case is

$$\widehat{\phi}_1^{\cos} = b_m \frac{\cosh(\beta_m y)}{\cosh(\beta_m h_0)} \cos(\beta_m x) \,, \tag{9.14}$$

with b_m an arbitrary constant, and

$$\widehat{\phi}_2^{\cos} = B_m \left[\left(x - \tfrac{1}{2} L\right) - \frac{4 s_m^2}{L} \sum_{n=0}^{\infty} \frac{1}{\alpha_n^2 \sigma_{m,n}} \frac{\cosh(\alpha_n y)}{\cosh(\alpha_n h_0)} \cos(\alpha_n x) \right] , \tag{9.15}$$

with B_m an arbitrary constant. The eigenfunctions (9.14) and (9.15) are the analogues in the cosine representation of the resonant eigenfunctions (9.8) and (9.9). Noting that $k_0 L = 2m\pi$ at resonance (9.2), giving $k_0 = \beta_m$, and so the first eigenfunction (9.8) is

$$\begin{aligned}
\widehat{\phi}_1^{\text{vert}} &= \cos(k_0 x)\psi_0(y) \\
&= \cos(k_0 x) \tfrac{1}{N_0} \cosh(k_0 y) \\
&= \tfrac{1}{N_0} \cos(\beta_m x) \, \cosh(\beta_m y) \\
&= \tfrac{\cosh(\beta_m h_0)}{N_0} \tfrac{\cosh(\beta_m y)}{\cosh(\beta_m h_0)} \cos(\beta_m x) \\
&= \tfrac{\cosh(\beta_m h_0)}{N_0} \tfrac{1}{b_m} \widehat{\phi}_1^{\cos} \,.
\end{aligned}$$

Modulo a multiplicative constant, $\widehat{\phi}_1^{\text{vert}}$ and $\widehat{\phi}_1^{\cos}$ are equivalent. The eigenfunctions $\widehat{\phi}_2^{\text{vert}}$ and $\widehat{\phi}_2^{\cos}$ are also equivalent and this follows from the equivalence argument in §7.

9.3 Numerics of the resonant characteristic equation

Consider the full characteristic function Δ^{vert} with both products included. Then a $1:1$ resonance occurs when Δ^{vert} and its first derivative vanish (9.6).

In Figure 9 the function Δ^{vert} is plotted as a function of s. The first zero is simple, and the second zero is double since the curve is tangent to the horizontal axis. This second root is an example of the $1:1$ resonance. The parameter values are given in the caption.

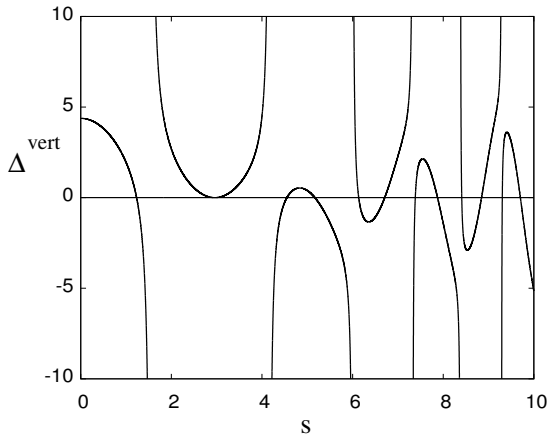

Figure 9: Plot of the characteristic function $\Delta^{\rm vert}(s)$ for $G = 4.376$, $R = 0.5$ and $\delta = 0.1$. The double root of the dispersion relation at $s = s_m = 2.958$ denotes a $1:1$ resonance.

10 Concluding remarks

To get some idea of the implications of the $1:1$ resonance for the nonlinear problem we can appeal to other problems with a $1:1$ resonance. The physical problem closest to the current model is the $1:1$ resonance in the Faraday experiment, when the vessel has a square or nearly-square horizontal cross-section. This configuration has been studied by Feng & Sethna [12]. The $1:1$ resonance is caused there by the square cross section, so physically it is very different from the mechanism for $1:1$ resonance here. However, mathematically it is very similar. To simplify notation, let

$$A := A_0^{(1)} \quad \text{and} \quad B := \widehat{\theta}\,.$$

Then the strategy for analyzing the weakly nonlinear problem is to introduce a slow time parameter

$$\tau = \varepsilon^2 t\,,$$

where ε is a measure of the amplitude of motion. Then let A and B depend on the slow time variable: $A(\tau)$ and $B(\tau)$. Then substitution into the nonlinear equations and carrying out an amplitude expansion leads to amplitude equations at third order of the form

$$\begin{aligned} {\rm i}A_\tau &= a_1 A + a_2|A|^2A + a_3|B|^2A + a_4B^2A \\ {\rm i}B_\tau &= b_1 B + b_2|B|^2B + a_3|A|^2B + a_4A^2B\,, \end{aligned} \tag{10.1}$$

with real parameters a_j, b_j. At resonance $a_1 = b_1$, and so $b_1 - a_1$ is a measure of the unfolding from resonance. According to results in [12] and [13] an analysis of solutions of this normal form shows that the weakly nonlinear solutions near resonance can be expected to include pure modes, mixed modes, secondary branches, connecting heteroclinic orbits, and heteroclinic cycles. Since A is associated with fluid motion and B is associated with vessel motion, a heteroclinic orbit is a mechanism for energy transfer between fluid and vessel.

Another example, which has similarities to the Cooker experiment, and shows how weakly nonlinear analysis near a resonance causes energy transfer between modes, is the

problem of a suspended elastic beam (Struble & Heinbockel [22]). In this model an elastic beam is suspended by two rigid cables free to rotate in the plane. The elastic beam is the analogue of the fluid in Cooker's experiment. The governing equations are quite different (for example the linearized equations completely decouple in [22]). However, there is a resonance, and their weakly nonlinear analysis shows that there are heteroclinic connections between solutions which are pathways to energy transfer.

Transfer of energy from non-symmetric to symmetric modes can also arise without resonance when forcing and nonlinearity are added. An example in the context of sloshing is the analysis of Zeng [26], where a modal expansion with one symmetric and one nonsymmetric mode under the influence of forcing is studied. This mechanism, and its analysis, is however very different from the internal resonance mechanism without forcing.

Acknowledgements

The authors are grateful to Professor Phil McIver of Loughborough University for suggesting the proof of equivalence [19] used in §7.

— Appendix —

A Resonance in the shallow water model

The characteristic equation with resonance is derived, starting with the linear shallow water equations with coupling (2.1). The coupling equation can be transformed to

$$\frac{d}{dt}\left[\int_0^L \rho h_0 u \,\mathrm{d}x + (m_v + m_f)\dot{q}\right] + \nu q = 0\,. \tag{A-1}$$

Now look for solutions that are periodic in time of frequency ω

$$h(x,t) = \widehat{h}(x)\cos(\omega t)\,, \quad u(x,t) = \widehat{u}(x)\sin(\omega t)\,, \quad q(t) = \widehat{q}\cos(\omega t)\,. \tag{A-2}$$

Substitution into the governing equations gives

$$-\omega\widehat{h} + h_0\widehat{u}_x = 0 \quad \text{and} \quad \omega\widehat{u} + g\widehat{h}_x = \omega^2\widehat{q}\,, \tag{A-3}$$

which when combined give

$$\widehat{u}_{xx} + \alpha^2\widehat{u} = \omega\alpha^2\,\widehat{q}\,, \quad \widehat{u}(0) = \widehat{u}(L) = 0\,, \quad \alpha = \frac{\omega}{\sqrt{gh_0}}\,. \tag{A-4}$$

The solution of (A-4) satisfying only the left boundary condition $\widehat{u}(0) = 0$ is

$$\widehat{u}(x) = A\,\sin(\alpha x) + \omega(1 - \cos(\alpha x))\widehat{q}\,,$$

where A is an arbitrary constant. Application of the second boundary condition $\widehat{u}(L) = 0$ gives

$$A\,\sin(2s) + 2s\sqrt{gh_0}(1-\cos(2s))\frac{\widehat{q}}{L} = 0\,. \tag{A-5}$$

There is a temptation to assume here that $\sin(s) \neq 0$ and then divide (A-5) by $\sin s$. However, $\sin(s)$ can be zero, so it should be retained.

Substitute the expression for $\widehat{u}$ into the vessel equation (A-1),

$$\frac{A}{2s}\,(1-\cos(2s)) + 2\sqrt{gh_0}\left[s - \frac{1}{2}\sin(2s)\right]\frac{\widehat{q}}{L} = 2\sqrt{gh_0}\left[(1+R)s - \frac{G}{s}\right]\frac{\widehat{q}}{L}\,. \tag{A-6}$$

Equations (A-5) and (A-6) are two homogeneous equations for two unknowns. Combining them into one matrix equation

$$\begin{bmatrix} \sin(2s) & 2s(1-\cos(2s)) \\ \dfrac{1}{2s}\,(1-\cos(2s)) & 2\left[\dfrac{G}{s} - Rs\right] - \sin(2s) \end{bmatrix} \begin{pmatrix} \dfrac{A}{\sqrt{gh_0}} \\ \dfrac{\widehat{q}}{L} \end{pmatrix} = \begin{pmatrix} 0 \\ 0 \end{pmatrix}\,.$$

For non-trivial solutions the determinant of the coefficient matrix must vanish, resulting in the characteristic equation

$$\Delta^{\mathrm{SW}}(s) = \det \begin{bmatrix} \sin(2s) & 2s(1-\cos(2s)) \\ \dfrac{1}{2s}\,(1-\cos(2s)) & 2\left[\dfrac{G}{s} - Rs\right] - \sin(2s) \end{bmatrix}\,,$$

or

$$\Delta^{\mathrm{SW}}(s) = 4\sin(s)\left[\left(\frac{G}{s} - Rs\right)\cos(s) - \sin(s)\right]\,.$$

However, if $\cos(s) = 0$ then $\Delta(s) = -4 \neq 0$. Hence $\cos(s)$ is never zero, and it can be divided out. Also dividing by 4 gives the characteristic equation (1.5).

B Nonlinear equations for Cooker's experiment

A schematic of the system is shown in Figure 10. There are two coordinate systems. The coordinates (X, Y) which are fixed in space, and placed at the suspension point of the left-most cable. The coordinates (x, y) are attached to the moving vessel. The relationship between the two coordinate systems is

$$X = x + q_1 \quad \text{and} \quad Y = y + q_2 - d\,, \tag{B-1}$$

with the constraint

$$q_1^2 + q_2^2 = \ell^2\,. \tag{B-2}$$

In polar coordinates, the position $\mathbf{q} = (q_1, q_2)$ is

$$q_1(t) = \ell\sin\theta(t) \quad \text{and} \quad q_2(t) = -\ell\cos\theta(t)\,. \tag{B-3}$$

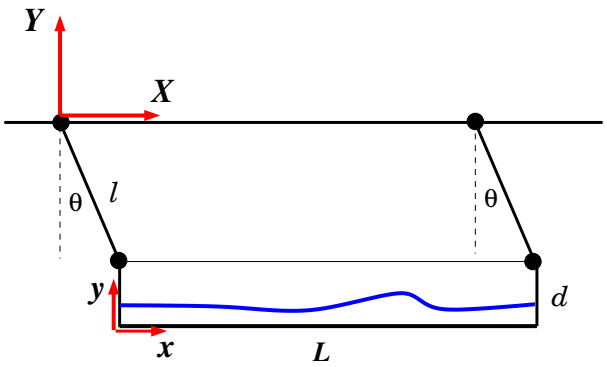

Figure 10: Schematic of Cooker's experimental configuration [9].

The fluid occupies the region

$$0 \le y \le h(x,t) \quad \text{with} \quad 0 \le x \le L\,,$$

and relative to the body frame the Eulerian fluid velocities are $u(x,y,t)$ and $v(x,y,t)$.

The governing equations for the fluid are the Euler equations relative to the body-fixed frame. A general derivation can be found in the papers [4, 5]. The Euler equations for the fluid relative to the body frame are

$$\begin{aligned} \frac{Du}{Dt} + \frac{1}{\rho}\frac{\partial p}{\partial x} &= -\ddot{q}_1 \\ \frac{Dv}{Dt} + \frac{1}{\rho}\frac{\partial p}{\partial y} &= -g - \ddot{q}_2\,, \end{aligned} \tag{B-4}$$

with

$$\ddot{q}_1 = \ell\cos\theta\,\ddot{\theta} - \ell\sin\theta\,\dot{\theta}^2 \quad \text{and} \quad \ddot{q}_2 = \ell\sin\theta\,\ddot{\theta} + \ell\cos\theta\,\dot{\theta}^2\,.$$

Accompanying these equations is conservation of mass relative to the body frame

$$\frac{\partial u}{\partial x} + \frac{\partial v}{\partial y} = 0\,. \tag{B-5}$$

The boundary conditions at the walls are

$$v = 0 \quad \text{at} \quad y = 0 \quad \text{and} \quad u = 0 \quad \text{at} \quad x = 0, L\,. \tag{B-6}$$

The boundary conditions at the free surface are

$$p = 0 \quad \text{and} \quad h_t + uh_x = v \quad \text{at} \quad y = h(x,t)\,. \tag{B-7}$$

The exact position of the vessel is determined by $\theta(t)$, and its governing equation is

$$\ddot{\theta} + \frac{g}{\ell}\sin\theta = \frac{1}{m_v \ell}\int_0^L \int_0^h (p_x\cos\theta + p_y\sin\theta)\,\mathrm{d}y\mathrm{d}x\,. \tag{B-8}$$

A derivation of this equation is given below in subsection B.1.

Another form for the vessel equation that will be of use is

$$\ddot{\theta} + \frac{g}{\ell}\sin\theta = -\frac{1}{(m_v + m_f)\ell}\left(\dot{c}_1\cos\theta + \dot{c}_2\sin\theta\right), \tag{B-9}$$

where $\mathbf{c} = (c_1, c_2)$ with

$$c_1 = \int_0^L \int_0^h \rho u \,\mathrm{d}y\mathrm{d}x \quad \text{and} \quad c_2 = \int_0^L \int_0^h \rho v \,\mathrm{d}y\mathrm{d}x\,. \tag{B-10}$$

The form of the equation (B-9) is derived by using the momentum equations (B-4) and the Reynold's transport theorem,

$$\dot{c}_1 = \frac{d}{dt}\int_0^L \int_0^h \rho u \,\mathrm{d}y\mathrm{d}x = \int_0^L \int_0^h \rho \frac{Du}{Dt}\,\mathrm{d}y\mathrm{d}x = \int_0^L \int_0^h (-p_x - \rho\ddot{q}_1)\,\mathrm{d}y\mathrm{d}x\,,$$

or

$$\dot{c}_1 + m_f\ddot{q}_1 = -\int_0^L \int_0^h p_x \mathrm{d}y\mathrm{d}x\,.$$

Similarly,

$$\dot{c}_2 + m_f(g + \ddot{q}_2) = -\int_0^L \int_0^h p_y \,\mathrm{d}y\mathrm{d}x\,.$$

Substitution of these two expressions into (B-9) and using $\ddot{q}_1\cos\theta + \ddot{q}_2\sin\theta = \ell\ddot{\theta}$ then gives (B-8).

B.1 Derivation of the vessel equation

The vessel equation (B-9) can be derived using a variational principle or directly using Newton's law. In this section the vessel equation is derived using a variational principle following Chapter 7 of Alemi Ardakani [2]. This equation can be independently confirmed by using Newton's law with constraints.

The kinetic energy of the system is

$$KE = \frac{1}{2}\int_0^L \int_0^h \rho[(u + \dot{q}_1)^2 + (v + \dot{q}_2)^2]\,\mathrm{d}y\mathrm{d}x + \frac{1}{2}m_v(\dot{q}_1^2 + \dot{q}_2^2)\,,$$

and the potential energy is

$$PE = \int_0^L \int_0^h \rho g(y - d + q_2)\,\mathrm{d}y\mathrm{d}x + \int\int_{vessel} \rho^{\text{vessel}} g(y - d + q_2)\,\mathrm{d}x\mathrm{d}y\,.$$

Let $\mathscr{L} = KE - PE$ and express q_1 and q_2 in terms of θ, and use the identities

$$m_f = \int_0^L \int_0^h \rho\,\mathrm{d}y\mathrm{d}x \quad \text{and} \quad m_v = \int\int_{vessel} \rho^{\text{vessel}}\,\mathrm{d}x\mathrm{d}y\,.$$

The Euler-Lagrange equation for θ is then

$$\begin{aligned}
\tfrac{d}{dt}\left(\tfrac{\partial\mathscr{L}}{\partial\dot{\theta}}\right) - \tfrac{\partial\mathscr{L}}{\partial\theta} &= \tfrac{d}{dt}\left((m_v + m_f)\ell^2\dot{\theta} + \ell c_1\cos\theta + \ell c_2\sin\theta\right) \\
&\quad - \left(-c_1\ell\sin\theta\dot{\theta} + c_2\ell\cos\theta\dot{\theta} - (m_v + m_f)g\ell\sin\theta\right) \\
&= (m_v + m_f)\ell^2\ddot{\theta} + \dot{c}_1\ell\cos\theta + \dot{c}_2\ell\sin\theta + (m_v + m_f)g\ell\sin\theta\,.
\end{aligned}$$

Dividing by $(m_v + m_f)\ell^2$ then confirms the form of the vessel equation (B-9).

This Lagrangian is quite satisfactory for deriving the equations for the vessel motion, but it does not give the correct equation for the fluid motion. The Lagrangian can be modified by adding constraints to give the fluid equations (see [2]), but a variational principal for the fluid motion will not be needed in this paper.

B.2 Irrotational flow and a velocity potential

Introduce a potential for the velocity field

$$u = \phi_x - \dot{q}_1 \quad \text{and} \quad v = \phi_y - \dot{q}_2 \,. \tag{B-11}$$

The fluid motion is now strictly irrotational since $v_x = u_y$ and mass conservation gives

$$\Delta\phi := \phi_{xx} + \phi_{yy} = 0 \,, \quad 0 < y < h(x,t) \,, \quad 0 < x < L \,. \tag{B-12}$$

Substitution of (B-11) reduces the momentum equations to the Bernoulli equation

$$\phi_t + \tfrac{1}{2}\left((\phi_x - \dot{q}_1)^2 + (\phi_y - \dot{q}_2)^2\right) + gy + \frac{p}{\rho} = b(t) \,,$$

for some function of time $b(t)$. Absorbing $b(t)$ into the velocity potential, and application of the boundary condition $p = 0$ at $y = h$ then gives the dynamic free surface boundary condition

$$\phi_t + \tfrac{1}{2}(\phi_x^2 + \phi_y^2) - \dot{q}_1\phi_x - \dot{q}_2\phi_y + gh + \tfrac{1}{2}(\dot{q}_1^2 + \dot{q}_2^2) = 0 \,, \quad \text{at} \quad y = h(x,t) \,. \tag{B-13}$$

The kinematic free surface boundary condition becomes

$$h_t + (\phi_x - \dot{q}_1)h_x = \phi_y - \dot{q}_2 \quad \text{at} \quad y = h(x,t) \,. \tag{B-14}$$

The boundary condition at the bottom is

$$\phi_y = \dot{q}_2 \quad \text{at} \quad y = 0 \,, \tag{B-15}$$

and at the sidewalls

$$\phi_x = \dot{q}_1 \quad \text{at} \quad x = 0, L \,. \tag{B-16}$$

For the vessel equation,

$$c_1 = \sigma_1 - m_f\dot{q}_1 \,, \quad \text{with} \quad \sigma_1 = \int_0^L \int_0^h \rho\phi_x \,\mathrm{d}y\mathrm{d}x \,,$$

and

$$c_2 = \sigma_2 - m_f\dot{q}_2 \,, \quad \text{with} \quad \sigma_2 = \int_0^L \int_0^h \rho\phi_y \,\mathrm{d}y\mathrm{d}x \,.$$

Substitution into the vessel equation (B-9) gives

$$m_v\ddot{\theta} + \frac{g}{\ell}(m_v + m_f)\sin\theta = -\frac{1}{\ell}\cos\theta\dot{\sigma}_1 - \frac{1}{\ell}\sin\theta\dot{\sigma}_2 \,. \tag{B-17}$$

In summary the governing equations for the nonlinear coupled problem in terms of the velocity potential are $\Delta\phi = 0$ in the interior, the free surface boundary conditions (B-13)-(B-14), the bottom and side wall boundary conditions (B-15)-(B-16), and the vehicle equation (B-17).

C The vertical eigenfunctions

The eigenvalue problem for the vertical eigenfunctions is recorded in (6.2) with λ the eigenvalue parameter, and ω^2/g is treated as a given real parameter. Here the properties of the eigenvalues and eigenfunctions are recorded following [18].

This eigenvalue problem can be solved analytically, but the characteristic equation for the eigenvalue λ is transcendental

$$\mathsf{C}(\lambda) = \frac{\omega^2 h_0}{g} \cos\left(h_0\sqrt{\lambda}\right) + \left(h_0\sqrt{\lambda}\right) \sin\left(h_0\sqrt{\lambda}\right). \tag{C-1}$$

The function $\mathsf{C}(\lambda)$ is real for all λ, $\mathsf{C}(0) > 0$ and $\mathsf{C}(\lambda) \to -\infty$ as $\lambda \to -\infty$. Hence there is at least one negative eigenvalue

$$\lambda_0 = -k_0^2 . \tag{C-2}$$

In fact, there is only one negative eigenvalue, and k_0 is the unique root of

$$k_0 h_0 \tanh(k_0 h_0) - \frac{\omega^2 h_0}{g} = 0 , \tag{C-3}$$

for any fixed $\omega^2 h_0/g$. The mode k_0 is associated with the *wave mode*.

In addition there is a countable number of positive eigenvalues

$$\lambda_n = k_n^2 , \quad n = 1, 2, \dots , \tag{C-4}$$

(see Figure 2.1 in [18]) with the sequence k_n determined by

$$k_n h_0 \tan(k_n h_0) + \frac{\omega^2 h_0}{g} = 0 , \quad n = 1, 2, \dots . \tag{C-5}$$

The modes k_n for $n \ge 1$ are associated with *evanescent modes*.

The associated eigenfunctions are

$$\psi_0(y) = \frac{1}{N_0} \cosh(k_0 y) \quad \text{and} \quad \psi_n(y) = \frac{1}{N_n} \cos(k_n y) , \quad n = 1, 2, \dots , \tag{C-6}$$

with

$$N_0 = \sqrt{\frac{1}{2}\left(1 + \frac{\sinh 2k_0 h_0}{2k_0 h_0}\right)} \quad \text{and} \quad N_n = \sqrt{\frac{1}{2}\left(1 + \frac{\sin 2k_n h_0}{2k_n h_0}\right)} . \tag{C-7}$$

The coefficients N_0 and N_n are chosen so that the eigenfunctions have unit norm,

$$\frac{1}{h_0}\int_0^{h_0} \psi_n(y)^2 \, \mathrm{d}y = 1 , \quad n = 0, 1, 2, \dots . \tag{C-8}$$

The set $\{\psi_0(y), \psi_1(y), \dots\}$ is complete on the interval $[0, h_0]$. Hence any square-integrable function $g(y)$ on this interval can be expanded in a series

$$g(y) = \sum_{n=0}^{\infty} g_n \psi_n(y) , \tag{C-9}$$

with the coefficients determined using orthogonality of the eigenfunctions,

$$g_n = \frac{1}{h_0}\int_0^{h_0} g(y)\, \psi_n(y) \, \mathrm{d}y . \tag{C-10}$$

References

[1] http://personal.maths.surrey.ac.uk/st/T.Bridges/SLOSH/

[2] H. Alemi Ardakani. *Rigid-body motion with interior shallow-water sloshing*, PhD Thesis, Department of Mathematics, University of Surrey (2010).

[3] H. Alemi Ardakani & T.J. Bridges. *Dynamic coupling between shallow-water sloshing and horizontal vehicle motion*, Euro. J. Appl. Math. **21** 479–517 (2010).

[4] H. Alemi Ardakani & T.J. Bridges. *Shallow-water sloshing in vessels undergoing prescribed rigid-body motion in three dimensions*, J. Fluid Mech. **667** 474–519 (2011).

[5] H. Alemi Ardakani & T.J. Bridges. *Shallow-water sloshing in vessels undergoing prescribed rigid-body motion in two dimensions*, Euro. J. Mech. B/Fluids **31** 30–43 (2012).

[6] H. Alemi Ardakani, T.J. Bridges & M.R. Turner. *Details of the proof of equivalence: the "cosine" versus "vertical eigenfunction" representations*, Technical Report, University of Surrey (2012). Electronic copy available at [1].

[7] J.P. Boyd. *Chebyshev and Fourier Spectral Methods*, Second Edition, Dover Publications: New York (2001).

[8] P.G. Chamberlain & D. Porter. *On the solution of the dispersion relation for water waves*, Appl. Ocean. Res. **21** 161–166 (1999).

[9] M.J. Cooker. *Water waves in a suspended container*, Wave Motion **20** 385–395 (1994).

[10] O.M. Faltinsen & A.N. Timokha. *Sloshing*, Cambridge University Press (2009).

[11] J.B. Frandsen. *Numerical predictions of tuned liquid tank structural systems*, J. Fluids & Structures **20** 309–329 (2005).

[12] Z.C. Feng & P.R. Sethna. *Symmetry breaking bifurcations in resonant surface waves*, J. Fluid Mech. **199** 495–518 (1989).

[13] Z.C. Feng & P.R. Sethna. *Global bifurcation and chaos in parametrically forced systems with* 1 : 1 *resonance*, Dynamical Systems: an Inter. Journal **5** 201–225 (1990).

[14] E.W. Graham & A.M. Rodriguez. *The characteristics of fuel motion which affect airplane dynamics*, J. Appl. Mech. **19** 381–388 (1952).

[15] A. Herczyński & P.D. Weidman. *Experiments on the periodic oscillation of free oscillations driven by liquid sloshing*, J. Fluid Mech. **693** 216–242 (2012).

[16] R.A. Ibrahim. *Liquid Sloshing Dynamics*, Cambridge University Press (2005).

[17] T. Ikeda & N. Nakagawa. *Non-linear vibrations of a structure caused by water sloshing in a rectangular tank*, J. Sound Vibr. **201** 23–41 (1997).

[18] C.M. Linton & P. McIver. *Handbook of Mathematical Techniques for Wave-Structure Interaction*, Chapman & Hall/CRC: Boca Raton (2001).

[19] P. McIver. Private Communication (2012).

[20] H. Ockendon, J.R. Ockendon & D.D. Waterhouse. *Multi-mode resonances in fluids*, J. Fluid Mech. **315** 317–344 (1996).

[21] H. Ockendon & J.R. Ockendon. *Nonlinearity in fluid resonances*, Meccanica **36** 297–321 (2001).

[22] R.A. Struble & J.H. Heinbockel. *Resonant oscillations of a beam-pendulum system*, J. Appl. Mech. **30** 181–188 (1963).

[23] G.I. Taylor. *The interaction between experiment and theory in fluid mechanics*, Ann. Rev. Fluid Mech. **6** 1–17 (1974).

[24] J.-M. Vanden-Broeck. *Nonlinear gravity-capillary standing waves in water of arbitrary uniform depth*, J. Fluid Mech. **139** 97–104 (1984).

[25] J. Yu. *Effects of finite water depth on natural frequencies of suspended water tanks*, Stud. Appl. Math. **125** 373–391 (2010).

[26] Z.C. Feng. *Coupling between neighboring two-dimensional modes of water waves*, Phys. Fluids **10** 2405–2411 (1998).